Infrared Generation by Coherent Excitation of Polaritons*

F. De Martini
Istituto di Fisica "G. Marconi," Universitá di Roma, Roma, Italy
(Received 12 April 1971)

The work presents a transient theory of the propagation in a cubic crystal of a polariton wave excited by a three-wave nonlinear parametric interaction. The coupling coefficient of the mixing process is calculated using a quantum-mechanical perturbation approach in the second-quantization formulation and including explicitly in the theory the phase and momentum mismatches of the interaction. The solution of the partial differential equations describing the evolution of the driving optical pulses leads to a complete formulation of the transient problem for the polariton pulse propagation. The transient problem is fully solved in the case in which the duration of the driving pulse $f(z,t)$ of the polariton wave is larger than the damping parameter Γ^{-1}: a case of general physical relevance including the optical behavior of short pulses generated by mode-locked lasers. In particular the solution of the problem leads to the definition of a characteristic interaction length and time depending on the initial conditions and affecting in a critical way the efficiency of the "coherent excitation" process. The Raman mixing process is briefly discussed as a particular case of the polariton process. The process of infrared generation is then taken into account on a semiclassical basis, with particular emphasis on the discussion of the propagation effects of the boundary conditions. In particular, the inhomogeneous character of the free solutions of the propagation equations is discussed. The theory is further extended to a brief discussion of the nonlinear optical behavior of the reststrahl band, leading to the consideration of an infinite nonlinear backward reflectivity at $\omega = \omega_{LO}$. An experiment is then described in which the coherent infrared generation in a crystal of gallium phosphide is applied to a series of accurate measurements of the linear and nonlinear optical parameters in the polariton region. The angular distribution of the emitted infrared intensity at wavelengths $\lambda = 29.2$, 29.9, and 34.6 μ and the spatial evolution of the polariton field in the quasicollinear kinematical configuration lead to the determination of the index of refraction of the crystal at these wavelengths and to the first direct measurement of the absorption coefficient in the zone of large polariton dispersion. On the basis of our results, we could verify the correctness of the multiple-oscillator theoretical model proposed by Barker in order to describe the lattice oscillation in GaP. Finally, the infrared intensity at the various frequencies leads to the determination of the dispersion of the modulus of the nonlinear optical susceptibility $|d|$ of the crystal. Assuming in first approximation a single-oscillator model for the lattice in the nonlinear regime, we could measure the characteristic nonlinear parameter $C = S(d_Q'/d_E')$. We found $C = -0.48 \pm 0.01$. The experimental methods described in the present work are of general interest for the nonlinear spectroscopy of solids in the optical and infrared range of frequencies.

I. INTRODUCTION

The coherent excitation of infrared- (ir) active transverse optical phonon modes in crystals by a three-wave nonlinear optical parametric process was considered by several theoretical workers soon after stimulated Raman scattering was discovered.[1-5] The main interest that was attracted by this effect in the early years of nonlinear optics was related to the possibility of achieving by nonlinear mixing the generation of coherent radiation at ir and far-infrared frequencies that were not made available at that time by other types of lasers. In more recent times the interest manifested by a large class of physicists in the study of the nonlinear optical properties of solids and, in particular, in the quantitative calculation, on a quantum-mechanical basis, of the nonlinear susceptibilities of crystals[6] has suggested the use of the nonlinear parametric effects in order to measure physical parameters that cannot be easily measured or are totally inaccessible to the usual methods of linear optics.

The coherent excitation of polaritons[7] by a parametric process has been recently achieved by beating two externally generated optical beams in the crystal[8] and by exciting a stimulated Raman scattering process directly in the medium.[9-11] In Refs. 8, 10, and 11 the excitation was detected by the observation, in the optical range, of the corresponding scattering, while in Ref. 9 the ir radiation associated with the excitation was detected in a non-phase-matching condition. Both methods, optical scattering and ir generation, are in general useful and, in some sense, complementary, when they are applied to the measurement of optical pa-

rameters of crystals. As far as we can judge from our experience in Ref. 8 (in which a double-scattering process was involved) and in the present work, the direct detection of the ir frequency gives, in general, more precise results in the collinear or nearly-collinear kinematical configuration, i.e., when the wave vectors $\vec{k}_1$ and $\vec{k}_2$ of the interacting optical beams at frequencies ω_1 and ω_2 are parallel or nearly parallel to the wave vector of the generated ir wave at frequency $\omega_3 = \omega_1 - \omega_2$. In cubic crystals having only one transverse optical mode, as in III-V semiconductors, that condition corresponds in general to the excitation of substantially photonlike polaritons.[12,13] On the other hand, for ω_3 approaching ω_{TO}, i.e., in a zone of phononlike polaritons, the experiment of ir generation becomes increasingly difficult owing mainly to the need of avoiding radiation trapping by total internal reflection in a crystal of increasing index of refraction. In that case, our method reported in[8] and based on an up-conversion scattering in the optical range is in general of easier application.

In the present work[14] we give first an extended theoretical account of the polariton propagation in a cubic crystal, starting from a very general transient theory of the nonlinear mixing process that should be of interest for the modern nonlinear optics of subnanosecond pulses. In Sec. III we consider more specifically the process of ir generation on a semiclassical basis, including detailed considerations on the propagation processes arising at the boundaries of the medium and leading to the creation of nonlinearly reflected and transmitted inhomogeneous waves. The theory is extended to the consideration of the nonlinear mixing process in the reststrahl band. In Secs. V, VI, and VII we describe an experiment in which two optical fields are made to interact in a III-V semiconductor GaP crystal where a coherent polariton field is created. The experimental determination of the spatial evolution of the polariton field in a quasicollinear configuration and the angular distribution of the emitted ir field outside the crystal lead to some precise measurements of the index of refraction of the crystal and of the absorption coefficient. Furthermore, the frequency dependence of the emitted ir intensity allows the study of the dispersion of the nonlinear optical susceptibility of the crystal near the reststrahl band.

The present work could be somewhat related to some ir difference-frequency generation experiments reported previously in the literature.[15-20] In these works the idler ir frequency that is excited in the coherent scattering is nevertheless so far from the lattice TO frequency that no polaritons can be thought to be excited. In these works and in the works previously quoted, no measurements similar to ours on the crystal parameters are reported.

II. TRANSIENT THEORY OF THE POLARITON WAVE PROPAGATION

The parametric difference-frequency generation process involving the scattering of a coherent polariton wave may be described starting either from the classical coupled-wave theory, of large use in nonlinear optics,[12,21] or from a quantum transition-rate formulation. The theory of the gain affecting the "signal" (optical) wave in a parametric process in which the frequency of one of the interacting fields is near a lattice resonance has been considered by Shen,[3] Butcher, Loudon, and McLean,[4] and, more recently, by Henry and Garrett[22] following the classical approach. The application of the classical method, which is usually concerned with em fields rather than energy flows, becomes nevertheless quite difficult when a complete description of the dynamics of a three-wave interaction is required. In order to overcome serious mathematical problems, some approximations are usually introduced in the theory, e.g., the lack of the depletion of the pump and the *a priori* hypothesis of an exponential gain solution for the waves.

As we shall see in the present section, these approximations are indeed not appropriate to a transient analysis of our process involving polariton particles rather than photons.

In the present section we start from a transition-rate approach and we shall develop a transient theory for the propagation of the interacting waves with particular emphasis on the growth of the polariton wave, a problem that has not been adequately considered in previous papers. We shall make use through this section of the useful notation of Refs. 22 and 23.

The polariton field states, in the linear approximation, will be considered as linear superpositions of the states of the electric field $\vec{E}_q$ and those of the lattice wave $\vec{Q}$, which are coupled together through the polarization of the crystal.[7,24]

The dynamics of our parametric process may be described by introducing a classical phenomenological free-energy density[8,12,23] $U(\vec{E}_1(\omega_1), \vec{E}_2(\omega_2), \vec{E}_q(\omega_3), \vec{Q}(\omega_3))$ written as a function of the interacting electric fields at frequencies ω_1, ω_2, $\omega_3 = \omega_1 - \omega_2$ and of the relative displacement $\vec{Q}(\omega_3)$ of the positive and negative sublattices caused by the phonons. The nonlinear coupling coefficients that appear in the expression of U may be taken as two tensor quantities, d_E and d_Q, that account, respectively, for the pure optical coupling via the electronic structure of the crystal and for the Raman-type coupling involving the optical phonon[22,25]

As long as we limit ourselves to considering a negligible change of population of the phonon state, the fields may be expressed in terms of boson

creation and annihilation operators $b^{\dagger}_{k_i}$, b_{k_i}. These operators satisfy the commutation relations[26]

$$[b_{k_i}, b^{\dagger}_{k_j}] = \delta_{k_i,k_j} \quad (i,j=1,2,3) \ . \tag{1}$$

If m_{k_1}, m_{k_2}, m_{k_3} are the mode occupation numbers for the three fields, the matrix elements of these operators in the Foch space are[26]

$$\begin{aligned} &\langle m_{k_i}-1 \,|\, b_{k_j} \,|\, m_{k_j}\rangle = m_{k_i}^{1/2}\delta_{k_i,k_j} \ , \\ &\langle m_{k_i}+1 \,|\, b^{\dagger}_{k_j} \,|\, m_{k_j}\rangle = (m_{k_i}+1)^{1/2}\delta_{k_i,k_j} \ . \end{aligned} \tag{2}$$

In the above expressions the symbols k_i represent the momenta of the fields $\vec{k}_i$.

The fields, assumed to be monochromatic plane waves, may be written in the following form:

$$\begin{aligned} \vec{E}_1(\omega_1) &= \left(\frac{2\pi\hbar\omega_1^3}{k_1^2c^2V}\right)^{1/2}\vec{p}_1(b_{k_1}e^{i\vec{k}_1\cdot\vec{r}} + b^{\dagger}_{k_1}e^{-i\vec{k}_1\cdot\vec{r}}) \ , \\ \vec{E}_2(\omega_2) &= \left(\frac{2\pi\hbar\omega_2^3}{k_2^2c^2V}\right)^{1/2}\vec{p}_2(b_{k_2}e^{i\vec{k}_2\cdot\vec{r}} + b^{\dagger}_{k_2}e^{-i\vec{k}_2\cdot\vec{r}}) \ , \\ \vec{E}_q(\omega_3) &= \left(\frac{2\pi\hbar\omega_3 v_p v_g}{c^2V}\right)^{1/2}\vec{p}(b_{k_3}e^{i\vec{k}_3\cdot\vec{r}} + b^{\dagger}_{k_3}e^{-i\vec{k}_3\cdot\vec{r}}) \ , \\ \vec{Q}(\omega_3) &= (4\pi N\mu\omega_0^2)^{-1/2}(c^2/v_p v_g - \epsilon_\infty)^{1/2}\vec{E}_q(\omega_3) \ . \end{aligned} \tag{3}$$

In the above expressions V is a volume of the solid with linear dimensions small compared to the inverse of the absorption coefficient $\alpha(\omega_3)$, N is the volume density of the primitive cells of the crystal, v_p and v_g are, respectively, the phase and the group (energy) velocity of the undamped polariton wave, μ is the reduced mass of the ionic oscillator relative to one primitive cell and associated with the TO lattice mode at frequency $\omega_{TO} \equiv \omega_0$, ϵ_∞ is the high-frequency dielectric constant of the crystal. The expressions of $v_g(\omega_3)$ and $v_p(\omega_3)$ $\equiv (\omega_3/|\vec{k}_3(\omega_3)|)$ may be obtained using the Huang polariton dispersion theory in the Lorentz oscillators model approximation.[24,27] In writing Eq. (3) we have assumed that the medium does not exhibit appreciable optical dispersion at the optical frequencies ω_1 and ω_2. The coefficients of the expressions of the polariton field $\{\vec{E}_q, \vec{Q}_q\}$ appearing in Eq. (3) have been first obtained by Loudon[1] by equating two equivalent expressions of the Poynting vector associated with a transverse em wave traveling in a highly dispersive medium (Refs. 28 and 29).

Allowing for a phase mismatch of the waves, $\Delta\vec{k} = \vec{k}_1 - \vec{k}_2 - \vec{k}_3'$ ($\vec{k}_3 = \vec{k}_3' + i\vec{k}_3''$), an interaction Hamiltonian density for the coupled fields system may be expressed in the following form:

$$\mathcal{H}_i = A\vec{p}_1\vec{p}_2\vec{p}_3 : \underline{d}(b_1b_2^{\dagger}b_3^{\dagger}e^{i\Delta\vec{k}\cdot\vec{r}} + b_1^{\dagger}b_2b_3e^{-i\Delta\vec{k}\cdot\vec{r}}) \ , \tag{4}$$

where A is a constant to be determined on the basis of the coefficients of the fields of (3) and $\underline{d}$ is the nonlinear susceptibility tensor that accounts for the coupling. A significant expression for the nonzero elements of $\underline{d}$ near the TO resonance has been given by Faust and Henry[23] in the form $\underline{d} = \underline{d}_E(1 + c\omega_0^2D^{-1})$, where $C = e^*N\underline{d}_Q/\mu\omega_0^2\underline{d}_E$ is a tensor parameter that characterizes the nonlinear response of the crystal,[25] e^* is the effective ionic charge of the lattice oscillators, and $D = \omega_0^2 - \omega^2 - i\omega\Gamma$, Γ being the damping parameter of the oscillator. Γ is frequency independent in the Lorentz oscillators model approximation.[24]

The interaction Hamiltonian H_I is found by integrating $\mathcal{H}_i$ over the volume V. If we consider one initial state $|m_{k_1}, m_{k_2}, m_{k_3}\rangle$ for the fields, then the transition probability, over a unit frequency range, per unit time, and corresponding to the scattering of a pump photon, is given by the following expression[30-32]:

$$\begin{aligned} w = \frac{4\pi^2}{\hbar^2}\,(&|\langle m_{k_1}-1, m_{k_2}+1, m_{k_3}+1 \,|\, H_I \,|\, m_{k_1}, m_{k_2}, m_{k_3}\rangle|^2 \\ &- |\langle m_{k_1}+1, m_{k_2}-1, m_{k_3}-1 \,|\, H_I \,|\, m_{k_1}, m_{k_2}, m_{k_3}\rangle|^2)\,\frac{\frac{1}{2}\alpha(\omega_3)}{|\Delta\vec{k}|^2 + [\frac{1}{2}\alpha(\omega_3)]^2}\,\delta(\Delta\omega) \ , \end{aligned} \tag{5}$$

where $\Delta\omega = (\omega_1 - \omega_2 - \omega_3)$ and $\alpha(\omega_3) = 2|\vec{k}_3''(\omega_3)|$ is the absorption coefficient. The Lorentzian factor depending on $\Delta\vec{k}$ and appearing in Eq. (5) accounts for the damping of the final polariton momentum state that is characterized by the absorption coefficient α. The explicit evaluation of this factor is reported in Appendix A.

Similarly the damping affecting the final energy state of the interaction is characterized by a frequency-dependent damping parameter $\tilde{\Gamma}(\omega_3)$ that is related to $\alpha(\omega_3)$ through the polariton group velocity:

$$\tilde{\Gamma}(\omega_3) = v_g(\omega_3)\alpha(\omega_3) \ . \tag{6}$$

Making use of Eq. (2), w becomes

$$\begin{aligned} w = \frac{B}{V}\,&\frac{(\frac{1}{2}\alpha)^2}{|\Delta\vec{k}|^2 + (\frac{1}{2}\alpha)^2}\,\delta(\Delta\omega) \\ &\times[m_{k_1}(m_{k_2} + m_{k_3} + 1) - m_{k_2}m_{k_3}] \ , \end{aligned} \tag{7}$$

where

$$B=\frac{32\pi^5\hbar\omega_2^3\omega_3^3\omega_1^3 v_p v_g |d|^2}{|\vec{k}_1|^2|\vec{k}_2|^2 c^6} \quad . \tag{7'}$$

In view of the discussion of our experiment that deals with a cubic crystal (GaP) belonging to the $\bar{4}3m$ class, we have omitted in (7') the tensor notation for the nonlinear coupling coefficient d. Hereafter we shall consider d, d_E, d_Q as scalar quantities because, for the given symmetry and crystal class, these tensors are determined by only one parameter.[33]

By integrating Eq. (7) over the distribution of the final-energy states we obtain the transition probability per unit time[31,32]:

$$W=\frac{B}{\pi^2 v_g V}\frac{(\frac{1}{2}\tilde{\Gamma})^2}{(\Delta\omega)^2+(\frac{1}{2}\tilde{\Gamma})^2}\frac{(\frac{1}{2}\alpha)^2}{|\Delta\vec{k}|^2+(\frac{1}{2}\alpha)^2} \times[m_{k_1}(m_{k_2}+m_{k_3}+1)-m_{k_2}m_{k_3}] \quad . \tag{8}$$

Expression (8) is valid for $\Delta\omega$ and $|\Delta\vec{k}|$ not too much larger than the corresponding damping parameters $\tilde{\Gamma}$ and α.

As will be shown later in the present section, the polariton density is much smaller than the photon densities at frequencies ω_1 and ω_2. Hence, for $m_{k_3}\gg 1$ we can write a simplified expression of W in the form

$$W=\frac{g m_{k_1} m_{k_2}}{V} \quad , \tag{9}$$

where

$$g\equiv\frac{B}{\pi^2 v_g}\frac{(\frac{1}{2}\alpha)^2}{|\Delta\vec{k}|^2+(\frac{1}{2}\alpha)^2}\frac{(\frac{1}{2}\tilde{\Gamma})^2}{(\Delta\omega)^2+(\frac{1}{2}\tilde{\Gamma})^2} \quad . \tag{9'}$$

A perturbation approach similar to the one reported above has been previously adopted in the context of scattering problems by Loudon[30] and in the work[22] without considering the phase mismatch $\Delta\vec{k}$ in the quantum-mechanical derivation of W.

As we shall verify later in the paper, our simple derivation of W and g as functions of $\Delta\vec{k}$ and $\Delta\omega$ leads us, in a straightforward way, to the correct expression of the (phase-mismatch dependent) intensity of the polariton wave $\rho_q(\omega_3)$. The $\Delta\vec{k}$ and $\Delta\omega$ dependence of $\rho_q(\omega_3)$ is at the basis of the general method of spectroscopy in the momentum space that has been recently introduced in solid-state optics.[8] Furthermore if we had applied our analysis to the derivation of the expression of the gain of the optical parametric oscillator, we would have found the correct dependence of that quantity on $|\Delta\vec{k}|$ and $(\Delta\omega)$ without recourse to the coupled-wave theory. As we have previously noticed, the above results are valid in the approximation of small momentum and frequency mismatches. For $\Delta\omega\gg\tilde{\Gamma}(\omega_3)$ and $|\Delta\vec{k}|\gg\alpha(\omega_3)$, as in reststrahl band propagation (cf. Sec. IV), the classical coupled-wave theory must be used.[5,12,22]

We consider in the present section a collinear interaction of the fields along the direction $\vec{z}$ normal to the entrance face of the crystal. The fields are written as functions of the corresponding z coordinate, having positive values in the crystal and being zero at the surface.

We also consider, in this section, a phase-matched interaction. The equations describing the evolution of the densities of the pump photons $\rho_1(z,t)\equiv(m_{k_1}/V)$ and of the Stokes photons $\rho_2(z,t)\equiv(m_{k_2}/V)$ may be written, owing to (9), in the following form:

$$\frac{\partial\rho_2}{\partial t}+v_2\frac{\partial\rho_2}{\partial z}=-\left(\frac{\partial\rho_1}{\partial t}+v_1\frac{\partial\rho_1}{\partial z}\right)=g\rho_1\rho_2 \quad , \tag{10}$$

where v_1 and v_2 are the group velocities of the two waves. For negligible optical dispersion of the medium at the frequencies ω_1 and ω_2 we have $v_1=(c/n_1)$ and $v_2=(c/n_2)$ where n_1 and n_2 are the refractive indices. Our present theory is greatly simplified if we set $v_1=v_2$ in Eq. (10). We will restore later the difference existing between v_1 and v_2 in the discussion of a simple condition of physical relevance in our experiment. We can now write the fields as functions of the propagation variables:

$$w_1=(t+z/v_1) \quad , \qquad \bar{w}_1=(t-z/v_1) \quad . \tag{11}$$

The corresponding inverse relations are $t=\frac{1}{2}(w_1+\bar{w}_1)$ and $z=(w_1-\bar{w}_1)\frac{1}{2}v_1$. A first integral of Eqs. (10) is given by the following expression:

$$\rho_1(w_1,\bar{w}_1)+\rho_2(w_1,\bar{w}_1)=f(\bar{w}_1) \quad . \tag{12}$$

The sum of the pump and Stokes pulses is a forward-propagating arbitrary function. We impose on the solution the following boundary condition: At $z=0$, $w_1=\bar{w}_1$, the ratio of the two fields is a prescribed function of time, $\rho_1(0,t)/\rho_2(0,t)=\epsilon(t)$. We rewrite that condition in the notation of the propagating frame, Eq. (11), and we make use of Eq. (12) in order to write the driving term $(\rho_1\rho_2)$ appearing in Eq. (10) as function of one of the fields. The solution of Eq. (10) is now straightforward. By restoring the initial variables but still keeping the useful notation $\bar{w}_1=(t-z/v_1)$, the fields are given in the following form:

$$\begin{aligned}\rho_1(z,t)&=f(\bar{w}_1)(1+e^{2G_1 f(\bar{w}_1)[z-\bar{z}(\bar{w}_1)]})^{-1} \quad ,\\ \rho_2(z,t)&=f(\bar{w}_1)(1+e^{-2G_1 f(\bar{w}_1)[z-\bar{z}(\bar{w}_1)]})^{-1} \quad ,\end{aligned} \tag{13}$$

and their product is given by

$$\rho_1(z,t)\rho_2(z,t)=[\tfrac{1}{2}f(\bar{w}_1)]^2\operatorname{sech}^2\{G_1 f(\bar{w}_1)[z-\bar{z}(\bar{w}_1)]\} \quad . \tag{14}$$

In the above expressions we have introduced the parameter $G_1=g/(2v_1)$ and the function $\bar{z}(\bar{w}_1)=[\ln\epsilon(\bar{w}_1)]/[2G_1 f(\bar{w}_1)]$ that accounts for the initial conditions.

A simple equation relates the Stokes to the pump field,

$$\rho_2(z, t) = \rho_1(z, t) \exp\{2G_1 f(\bar{w}_1)[z - \bar{z}(\bar{w}_1)]\} , \qquad (15)$$

showing an exponential growth for $\rho_2(z, t)$ when the pump field is considered undepleted by the interaction.[12]

The continuity equation for the polariton density $\rho_q(z, t) = (m_{k_3}/V)$ is given in the following form:

$$\frac{\partial \rho_q}{\partial t} + v_g \frac{\partial \rho_q}{\partial z} = g(\omega_3)\rho_1 \rho_2 - \tilde{\Gamma}'(\omega_3)\rho_q , \qquad (16)$$

where $\tilde{\Gamma}'(\omega_3)$ is a phenomenological "damping" parameter that accounts for the relaxation of the polaritons to the ground state. Making use of the notation of magnetic resonance,[34] we can associate $\tilde{\Gamma}'(\omega_3)$ with the longitudinal relaxation time T_1, and write $\tilde{\Gamma}'(\omega_0) = (1/T_1)$. We notice that, in general, $\tilde{\Gamma}'(\omega_0) \equiv \Gamma'$ is smaller than the parameter $\tilde{\Gamma}(\omega_0) \equiv \Gamma$ that appears in the expression of $g(\omega_0)$ given by Eq. (9′). In effect $\tilde{\Gamma}(\omega)$ is the linewidth of the polariton resonance and it is determined, competitively, by the inhomogeneous broadening process and by the effect of the coherence relaxation.[35] When this last effect is overwhelming, the linewidth of the TO resonance $\Gamma \equiv \tilde{\Gamma}(\omega_0)$ is approximately equal to the inverse of the transverse relaxation time T_2.[34] Obviously, the present considerations on the effects of the different homogeneous broadening processes are physically relevant only when we are dealing with quantum systems that are not too strongly coupled by collisions, e.g., excited molecules in a gas. In that case $T_2 \ll T_1$. For optical phonons in solids at normal temperature we can assume $T_1 \simeq T_2$.

In the present section we shall consider a driving pulse $f(\bar{w}_1)$ that is a regular analytical function of $\bar{w}_1$. Without lack of generality and for simplicity's sake we shall deal mainly with a symmetric pulse characterized by a time duration $\Delta\tau = (K')^{-1}$ that is approximately equal to the inverse of the time derivative of $f(\bar{w}_1)$, e.g., $f(\bar{w}_1) = \mathrm{sech}(K'\bar{w}_1)$.

An approximate analytical solution of Eq. (16), written in its most general form, may be easily worked out if we suppose $(\tilde{\Gamma}'/K') \gg 1$ and $(G_1 v_g/\tilde{\Gamma}') \ll 1$, as we will see.

In order to solve Eq. (16), we apply again a transformation of variables from the set $\{z, t\}$ to the propagation one $\{w, \bar{w}\}$, where $w = t + z/v_g$ and $\bar{w} = t - z/v_g$. The functions $f(\bar{w}_1)$ and $z(\bar{w}_1)$ appearing in Eq. (14) are now written in terms of the new variables according to the equation $\bar{w}_1 = \tilde{\alpha}w + \tilde{\delta}\bar{w}$, being $\tilde{\alpha} = (1 - \tilde{\beta})/2$, $\tilde{\delta} = (1 + \tilde{\beta})/2$, and $\tilde{\beta} = (v_g/v_1) \ll 1$.

In the new frame, Eq. (16) is a standard linear equation whose general solution may be expressed in the following integral form:

$$\rho_q(w, \bar{w}) = e^{-\tilde{\Gamma}' w/2}\left(C_2(\bar{w}) + (g/2)\int \rho_1 \rho_2 e^{\tilde{\Gamma}' w/2}\, dw\right), \qquad (17)$$

where $C_2(\bar{w})$ is an arbitrary function of $\bar{w}$, to be determined by the boundary conditions.

The exact analytical calculation of the integral $I(w, \bar{w}) = \int \rho_1 \rho_2 e^{\tilde{\Gamma}' w/2}\, dw$ is not possible in general when regular $f(\bar{w}_1)$ pulses of the type we have just described are inserted in Eq. (14). However, if $\tilde{\Gamma}' \gg K'$ and $\tilde{g} \equiv g\tilde{\beta} \ll \tilde{\Gamma}'$, the integral may be easily calculated by successive integrations by parts, at each step taking the exponential function of the integrand as the differential factor of the integration. We obtain in that way a rapidly converging series of functions whose terms are proportional to increasing powers of $\tilde{g}/\tilde{\Gamma}'$ and of $K'/\tilde{\Gamma}'$.

We can verify that the above assumptions are consistent with the conditions of our experiment to be discussed in Sec. V. In particular, as the linewidth of the TO resonance in gallium phosphide is about 4 cm^{-1} (Ref. 23), our present analysis is valid for pulse durations $\Delta\tau$ larger than $\sim 10^{-11}$ sec., viz., for pulses generated by the common mode-locked lasers.

If we now neglect, in the explicit expression of $I(w, \bar{w})$, the second and higher powers of $\tilde{g}/\tilde{\Gamma}'$ and $K'/\tilde{\Gamma}'$, we can write to a good approximation

$$I(w, \bar{w}) \simeq (2/\tilde{\Gamma}')\, e^{\tilde{\Gamma}' w/2}\,[f(\tilde{\alpha}w + \tilde{\delta}\bar{w})]^2 \times \mathrm{sech}^2\left[G_1 f(\tilde{\alpha}w + \tilde{\delta}\bar{w})\left(\frac{w - \bar{w}}{2} - \bar{z}(\tilde{\alpha}w + \tilde{\delta}\bar{w})\right)\right] . \qquad (18)$$

We determine $C_2(\bar{w})$ for a pulse $f(\bar{w}_1)$ of finite length, by imposing the condition $\rho_q(z, t) = 0$ at $t = -\infty$. The free solution of Eq. (16) disappears and the general solution is given by the following expression:

$$\rho_q(z, t) = \frac{g}{4\tilde{\Gamma}'}\left\{[f(\bar{w}_1)]^2 \mathrm{sech}^2[G_1 f(\bar{w}_1)(z - \bar{z}(\bar{w}_1))]\right\} , \qquad (19)$$

having kept again in Eq. (19) the notation $\bar{w}_1 = (t - z/v_1)$.

The time evolution of the solution (19) corresponding to the conditions $f(z, t) \equiv \mathrm{sech}[K(z - v_1 t)]$ and $\bar{z}(\bar{w}_1) = \mathrm{const}/[G_1 f(\bar{w}_1)]$ is shown in Fig. 1. We note that, in that case, the solution is represented by a pulse having a shape that is rapidly changing in time but that keeps quasistationary in space the position of its absolute maximum. For a regular symmetric pulse $f(\bar{w}_1)$ having its maximum at $\bar{w}_1 = 0$ and for $\bar{z}(\bar{w}_1)G_1 f(\bar{w}_1) \equiv \eta(\bar{w}_1) = \mathrm{const}$, the polariton density function reaches its absolute maximum at the coordinate $z = \bar{z}(0) = \eta/(G_1 f(0))$ and at the time $t = \bar{z}(0)/v_1$. For $t > \bar{z}(0)/v_1$, the polariton pulse spreads out in space at a rate proportional to the coupling parameter G_1. That same quantity determines the width of the zone of maximum $\rho_q(z, t)$, if the length of the pulse $f(\bar{w}_1)$ is larger than $[1/(G_1 f(0))]$, and it is proportional to the maximum value of $\rho_q(z, t)$ equal to $g/(4\tilde{\Gamma}')$. Obviously more

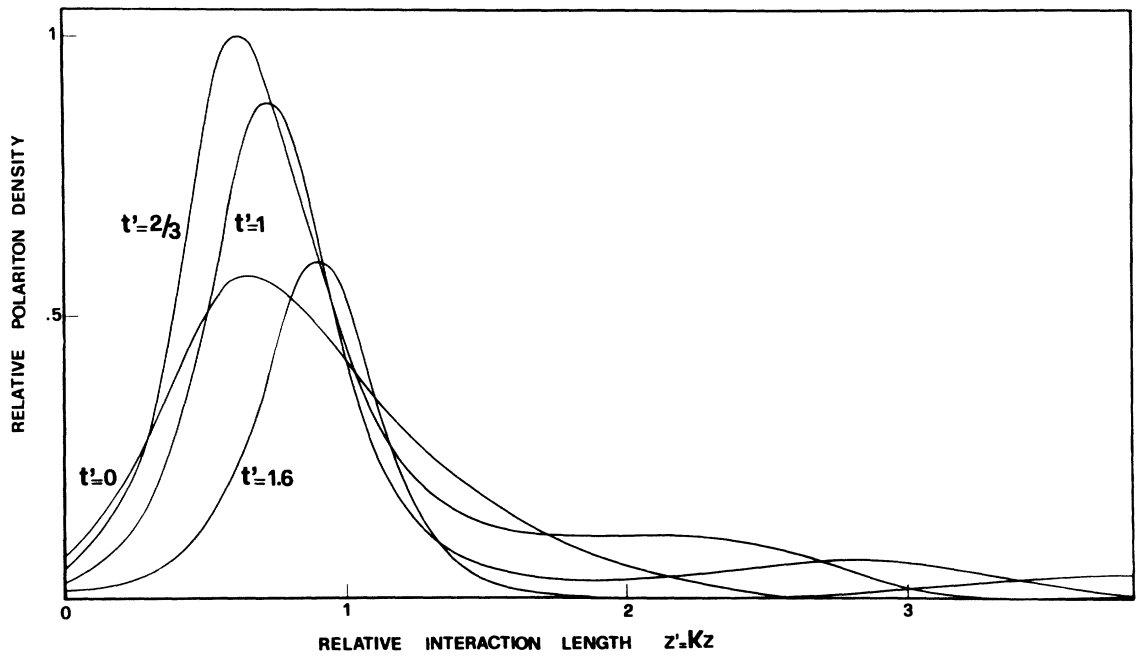

FIG. 1. Time evolution of the polariton density pulse ρ_q corresponding to the driving pulse $f(z,t)=\operatorname{sech} K(z-v_1t)$ and to the condition $\bar{z}(\bar{w}_1)=\eta/(G_1f(\bar{w}_1))$, η being constant. The above curves are drawn as functions of the dimensionless quantities $z'=Kz$, $t'=Kv_1t$ and they correspond to the following values of the parameters: $\eta=2$ and $G_1/K=3$. We note that the maximum value of ρ_q is reached at the time $t'=\eta K/G_1$ and at the coordinate $z'=\bar{z}'(0)=t'$.

complex situations arise when η is a variable function of $\bar{w}_1$.

Owing to the above considerations, we can conclude that the effect of ir generation with excitation of polaritons is a somewhat critical process in particular when short pulses (e.g., generated by mode-locked lasers) are made to interact in a highly nonlinear medium. Referring ourselves to the conditions corresponding to Fig. 1, we notice that the maximum value of $\rho_q(z,t)$ will never be reached during the interaction if the coordinate $\bar{z}(0)$, which depends on the amplitude of the optical fields before the interaction, lies outside the nonlinear crystal. Furthermore, when the ir pulse emitted from a crystal of length L is detected in the forward direction, the maximum efficiency of the ir generation process corresponds to the condition $\bar{z}(0)\simeq L$, viz., the exciting fields before the interaction must be related as follows: $\rho_1^0(\bar{w}_1)\simeq\rho_2^0(\bar{w}_1)\,e^{G_1f(0)L}$. Similarly, when the ir wave is detected in the backward direction owing to a process of nonlinear reflection from the entrance boundary located at $z=0$ (cf. Sec. III), the maximum ir efficiency corresponds to $\bar{z}(0)\simeq 0$ and $\rho_1^0(\bar{w}_1)\simeq\rho_2^0(\bar{w}_1)$.

A consequent extension of our theory, of particular interest for the nonlinear optics of ultrashort pulses, would be the analysis of the transient solution of Eq. (16) when the process we are considering is used for amplifying a short ir pulse injected in the medium together with the optical pulses. A discussion of that problem will not be undertaken here. We limit ourselves to noticing here that the consideration of the group velocity mismatch affecting the interaction of the ir and optical pulses leads to the addition of new restrictive conditions on several parameters of the process. For instance it is easy to prove that, by assuming an initial infinitely short ir pulse and the boundary conditions corresponding to Fig. 1, amplification is possible only if $L\lesssim 1/(G_1f(0))$. This additional condition leads to an upper limit to the amplification factor of the process.

In view of the discussion of our experiment it is worthwhile to discuss here the simple case in which $\epsilon(\bar{w}_1)=\text{const}$ and $f(\bar{w}_1)\equiv\rho^0=\text{const}$, i.e., the steady-state interaction of the fields. In that case Eqs. (10) and (16) may be easily solved without recourse to the simplifying hypothesis $n_1/n_2\equiv\xi=1$. In that case, if $\rho_1^0\equiv[\rho_1(z)]_{z=0}$, $\rho_2^0\equiv[\rho_2(z)]_{z=0}$, and $\rho^0=\rho_1^0+\xi\rho_2^0$ are the fields at the crystal boundary $z=0$, the solution of the set (10) is found to be

$$\rho_1(z)=\rho^0\{1+\exp[2G_2\rho^0(z-\bar{z})]\}^{-1},$$
$$\rho_2(z)=(\rho^0/\xi)\{1+\exp[-2G_2\rho^0(z-\bar{z})]\}^{-1}, \tag{20}$$

where $G_2=g/(2v_2)$ and $\bar{z}$ is a characteristic length of the interaction,

$$\bar{z}=(2G_2\rho^0)^{-1}\ln[\rho_1^0/(\xi\rho_0^2)],$$

which can be positive or negative depending on the

ratio of the boundary values of the fields. We may verify that at $z=\bar{z}$ the Stokes and the pump photon densities reach about half their asymptotic values and the driving function $\rho_1(z)\rho_2(z)$ is maximum. The general steady-state solution of the polariton density equation Eq. (16) is given by the following simple expression:

$$\rho_q(z)=\left(\frac{(\rho^0)^2 g}{4\xi\tilde{\Gamma}'}\right)\ \mathrm{sech}^2\{\rho^0 G_2(z-\bar{z})\}\ , \qquad (21)$$

showing clearly the effect of the boundary conditions, i.e., the sign and value of $\bar{z}$, on the efficiency of the parametric process.

The validity of the theory we have just discussed, which is based on a set of quantum rate equations, is limited to a dynamical condition corresponding to a value of the transition rate W [Eq. (8)] that is much smaller than the inverse of the transverse relaxation time T_2, i.e., Γ^{-1} in solids. If that condition is not satisfied, the perturbation approach of our quantum-mechanical formulation must be replaced by a more involved transient theory in which the harmonic oscillator model, which in the linear approximation accounts for the optical response of the medium, must be replaced by a fictitious-spin formulation leading to the solution of Bloch-type equations.[34,35]

The explicit expression for the maximum intensity $\bar{\rho}_q(\omega)$ of the polariton density distribution $\bar{\rho}_q(z,t)$ as a function of the ir frequency ω may be found by combining Eqs. (6), (7′), and (9′) and making use of the Huang polariton dispersion theory.[27]

By neglecting the damping in the expression of D and setting $D\simeq D'\equiv(\omega_0^2-\omega^2)$, $\bar{\rho}_q(\omega)$ may be given in the following form:

$$\bar{\rho}_q(\omega)=\bar{\rho}_q(\omega_0)\,\frac{[D'+C\omega_0^2]^2[D'^2+\beta\omega_0^4]}{C^2\beta\omega_0^5\omega^3}$$

$$\times\left\{\frac{[\tfrac{1}{2}\alpha(\omega)]^2}{|\Delta\vec{k}|^2[\tfrac{1}{2}\alpha(\omega)]^2}\,\frac{[\tfrac{1}{2}\tilde{\Gamma}(\omega)]^2}{(\Delta\omega)^2+[\tfrac{1}{2}\tilde{\Gamma}(\omega)]^2}\right\}\ , \qquad (22)$$

where

$$\bar{\rho}_q(\omega_0)=\frac{\pi\hbar\,\omega_1\omega_2\omega_0(\rho^0)^2}{2n_1^2n_2^2}\,\frac{Sd_Q'^2}{(\Gamma\Gamma')} \qquad (22')$$

is the maximum value of the optical phonon density distribution that is created in the medium, owing to a Raman-mixing process, when $(\omega_1-\omega_2)\simeq\omega_0\equiv\omega_{TO}$. We have introduced in expressions (22) and (22′) the strength of the lattice oscillator S, the parameters $\beta=(S/\epsilon_\infty)$ and $d_Q'=(d_Q/e^*)$. Furthermore we have assumed $\tilde{\Gamma}'(\omega_0)\equiv\Gamma'$, $\tilde{\Gamma}(\omega_0)\equiv\Gamma$, $\tilde{\Gamma}'(\omega)=[(\Gamma'/\Gamma)\tilde{\Gamma}(\omega)]$ and we have written $\tilde{\Gamma}(\omega)=\{\Gamma\beta\,\omega_0^2\omega^2\times[D'^2+\beta\omega_0^4]^{-1}\}$ owing to Eq. (6) and the Huang relations for $v_g(\omega)$ and $\alpha(\omega)$.[27] In Fig. 2 the frequency dependence of $\bar{\rho}_q(\omega)$ is shown for gallium phosphide in conditions of frequency and phase matching: $\Delta\omega=|\Delta\vec{k}|=0$. We note that $\bar{\rho}_q(\omega)$ reaches a minimum at the frequency $\tilde{\omega}=\omega_0\sqrt{1+C}$ owing to the effect of the negative interference between the electronic and ionic contributions to the nonlinear coupling coefficient $d=d_E[1+C\omega_0^2/D]$ appearing in Eq. (4). For gallium phosphide $C\simeq-0.48$ (cf. Ref. 23 and Sec. VII). Similar behavior is shown by the frequency dependence of the gain of a parametric oscillator when the frequency of the idler wave is near to the lattice resonance.[22]

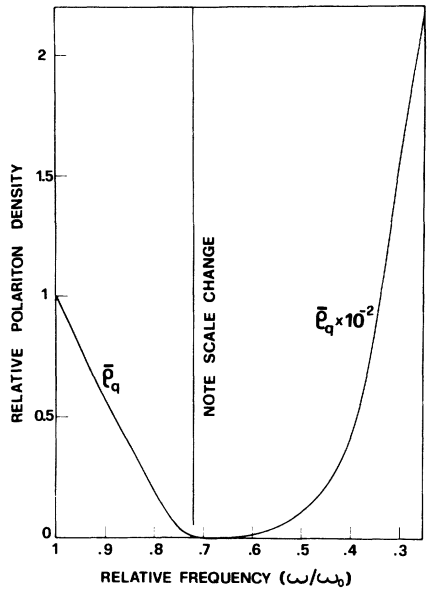

FIG. 2. Frequency dependence of the maximum value of the polariton density distribution in the crystal. The curve is drawn for GaP, for which the TO-mode frequency is $\omega_0\approx366\ \mathrm{cm}^{-1}$.

The general formulation in terms of polariton particles we have adopted in the present section has led us to build a transient propagation theory that applies entirely to the pure Raman interaction, $(\omega_1-\omega_2)=\omega_0$, even when the lattice (or molecular) oscillator is not ir active and $v_g\simeq0$ for every $\Delta\vec{k}=(\vec{k}_1-\vec{k}_2)$. In that case $\rho_q(z,t)$ has to be interpreted as the distribution of the density of optical phonons or of excited molecules. That phonon "wave packet" travels in the medium, as shown in Fig. 1, in spite of the condition of zero group velocity of the excitation.

As is well known, for pure Raman scattering of a non-ir-active excitation, the condition of phase matching $\Delta\vec{k}\simeq0$ is always satisfied and we can set $\alpha=0$ owing to Eq. (6). In that case, the maximum intensity of the phonon distribution may be conveniently expressed as function of the frequency mismatch $\Delta\omega=(\omega_1-\omega_2-\omega_3)$ in the following form:

$$\bar{\rho}_q(\omega)=\frac{\pi\hbar\,\omega_1\omega_2\omega_0(\rho^0)^2}{2n_1^2n_2^2}\,\frac{Sd_Q'^2}{(\Delta\omega)^2+\Gamma^2}\left(\frac{\Gamma}{\Gamma'}\right). \qquad (22'')$$

We notice that in writing Eq. (22″) we have partial-

ly neglected the effect of the damping of the lattice oscillator by having set $D = D'$ in Eq. (22). Making use of the complex expression of D in the derivation of $\bar{\rho}_q(\omega)$ would lead to a modification of Eq. (22″) that would be of physical relevance in connection with the discussion of some fine aspects of the coherent Raman interaction. Furthermore, we note that the validity of our results depends on the condition of a relatively large value of the relaxation parameter $\tilde{\Gamma}'(\omega)$, a condition that is generally verified for vibrational resonances in liquids and solids at normal temperature. It is not generally verified in gases at low pressure when a Q-switched laser pulse is used as the pump of the process. A recent measurement of $T_1 = (\Gamma')^{-1}$ for the $v = 1, j = 1$ vibrational level of the H_2 molecule has given a value $T_1 \simeq 10^{-3}$ sec at atmospheric pressure and normal temperature.[36]

We believe that the results of our present transient theory of the phonon-polariton propagation must be of large interest for the experimental application of the two-photon resonant mixing method of "coherent excitation"[5,8] to the measurement of physical parameters of Raman-active media. Besides the experiment to be discussed in the present work, the method of coherent excitation is at present being applied to the measurement of relaxation times in gases[5,36,37] and in solids.[8] Furthermore, it is at the basis of the experiments aimed toward the verification of the transient Raman-echo effect[38,39] that are presently in progress in several laboratories. The two-photon coherent excitation method is today one of the most useful applications of tunable lasers to the spectroscopy of Raman-active excitations in material media.

III. ir GENERATION

The formulation in terms of polarization particles adopted in Sec. II does not allow a complete description of the generated ir electromagnetic field in the medium. The above analysis must be completed by additional conditions that lead us to consider reflected and transmitted electromagnetic waves at the boundaries of the cyrstal at the fundamental frequencies ω_1 and ω_2 as well as at the frequency of the idler wave, ω_3. In the present section we shall consider, to the extent that would be apt to the discussion of our experiment (Sec. V), such effects with particular emphasis on the ones that originate specifically from the nonlinear behavior of the crystal. Furthermore, we shall deal with classical waves rather than photons in order to be able to take into account the phase of the fields and to consider in a more transparent way the kinematics of the process.

The problem of solving the nonlinear wave equations of a parametric process which satisfy the boundary conditions has been extensively considered by Bloembergen and Pershan[40] with particular emphasis on second harmonic generation and for a slightly dispersive medium. As the dispersive behavior of the linear and nonlinear optical response of the medium could be extremely pronounced in the polariton region, it is worthwhile to reconsider the problem for our difference-frequency generation process. We shall be led in particular to consider the inhomogeneous character of the transmitted and reflected waves in the medium that are nonlinearly generated at the boundaries.[41] Such are nonobvious processes of particular relevance in polariton optics. In the present section the notation of work[40] will be followed closely.

In view of our experimental conditions, we limit ourselves to considering in the present section a steady-state regime for the field—viz., the value of the interaction path L in the medium is supposed to be much smaller than the width of the driving pulse $f(\bar{w}_1)$ and of the value of the coupling parameter $[G_1 f(0)]^{-1}$. Furthermore, we make the simplifying hypothesis that the optical fields at frequencies ω_1 and ω_2 are not affected by the parametric "gain" process.

Using the notation of Ref. 23 the propagation equation of the polariton field at the frequency ω_3 may be written as follows[42]:

$$\left[\nabla^2 + \left(\frac{\omega_3}{c}\right)^2 \epsilon_\infty\right] \vec{E}_q(\omega_3) = -4\pi N e^* \left(\frac{\omega_3}{c}\right)^2 \vec{Q} - 4\pi \left(\frac{\omega_3}{c}\right)^2 \vec{P}^{NL}(\omega_3) , \quad (23)$$

$$\mu D(\omega_3) \vec{Q}(\omega_3) = e^* \vec{E}_q(\omega_3) + \vec{F}^{NL}(\omega_3) ,$$

where ϵ_∞ takes into account the linear response of the crystal free from the effect of the lattice resonance. $\vec{F}^{NL}(\omega_3)$ and $\vec{P}^{NL}(\omega_3)$ are, respectively, the nonlinear force and polarization that can be defined in terms of the nonlinear energy density U^{NL} in the following way:

$$\vec{P}^{NL}(\omega_3) = -\frac{\partial U^{NL}}{\partial \vec{E}_q^*(\omega_3)} , \quad \vec{F}^{NL}(\omega_3) = -\frac{\partial U^{NL}}{\partial [N\vec{Q}^*(\omega_3)]} . \quad (24)$$

According to Henry and Garrett[22] U^{NL} may be expressed in the following form:

$$U^{NL} = -[\underline{d}_E \vdots \vec{E}_1(\omega_1)\vec{E}_2^*(\omega_2)\vec{E}_q^*(\omega_3) + N\underline{d}_Q \vdots \vec{E}_1(\omega_1)\vec{E}_2^*(\omega_2)\vec{Q}^*(\omega_3) + \text{c.c.}] . \quad (25)$$

We verify that Eq. (25) is consistent with the definition of the Hamiltonian density given in Eq. (4). It has been shown by Garrett[25] that the tensor nonlinear coupling coefficients appearing in Eq. (25) may be taken as real and frequency independent over a large range of ir frequencies centered on

ω_0. As explained in Sec. II, we shall omit in our analysis the tensor notation for d_E and d_Q.

The complete solution of Eq. (23) is a linear superposition of the solutions of the homogeneous Maxwell equation, written in terms of the electric fields, and of the inhomogeneous one.

We consider, in the present section, the parametric excitation of a polariton wave in a nonlinear cubic crystal bounded by two plane faces that are not necessarily parallel. We assume that the linear medium in which the crystal is immersed has refractive index $n \simeq 1$ and that the optical fields $\vec{E}_1(\omega_1)$ and $\vec{E}_2(\omega_2)$ are undamped infinite plane waves interacting through the entire thickness of the crystal. They give rise, in the crystal, to a nonlinear polarization $\vec{P}^{NL}(\omega_3) = \vec{p} P^{NL}(\omega_3)$. In view of the conditions of our experiment, we limit ourselves to considering the case in which the (real) wave vectors $\vec{k}_1$ and $\vec{k}_2$ of the optical fields in the medium belong to the same incidence plane, which is orthogonal to the crystal boundaries, with $\vec{p}$ orthogonal to that plane.

A particular solution $\vec{E}_s(\omega_3)$ of Eq. (23) may be given in the following form[43]:

$$\vec{E}_s(\omega_3) = \frac{[d'_E + d'_Q(\omega_P^2/D)]\,|\,E_1 E_2^*\,|}{(k_s c/\omega_3)^2 - (\epsilon_\infty + \omega_P^2/D)} \left(\vec{p} - \frac{\vec{k}_s(\vec{k}_s\cdot\vec{p})}{k_s^2}\right) \times \exp[i(\vec{k}_s\cdot\vec{r} - \omega_3 t)] + \text{c. c.} \quad (26)$$

We have introduced in Eq. (26) the notation for the moduli of the vectors: $E_1 \equiv |\vec{E}_i|$, $k_i \equiv |\vec{k}_i|$, etc. In our particular case the term $\vec{k}_s(\vec{k}_s\cdot\vec{p}/k_s^2)$ is zero throughout the crystal. We have introduced in Eq. (26) the effective plasma frequency $\omega_P = (4\pi N e^{*2}/\mu)^{1/2}$; the wave vector of the driving polarization wave,

$$\vec{k}_s = (\vec{k}_1 - \vec{k}_2) \equiv (n_s\omega_3/c)(\vec{k}_s/k_s)\ (n_s^2 \equiv \epsilon_s);$$

and new symbols for the nonlinear coefficients[22]: $d'_E = 4\pi d_E$, $d'_Q = (d_Q/e^*)$.

The solution of the homogeneous Maxwell equation for the ir field near the entrance boundary is composed of a transmitted wave $\vec{E}_T(\omega_3)$, traveling in the nonlinear medium with wave vector $\vec{k}_T = \vec{k}'_T + i\vec{k}''_T$, and a nonlinearly reflected wave $\vec{E}_R(\omega)$ traveling in the backward direction, in the linear medium. Calling φ'_s, φ'_T, φ'_R the angles made by the $\vec{k}_s$, $\vec{k}_3 \equiv \vec{k}'_T$, $\vec{k}_R = n(\omega_3/c)\vec{k}_R/k_R$ wave vectors with the z axis defined as in Sec. II, the continuity of the transverse components of the momenta of the waves at the boundary leads to the generalized Snell equations,[40] $n_s \sin\varphi'_s = n_T \sin\varphi'_T = n \sin\varphi'_R$ being $n_T = n'_T(\omega_3) + in''_T(\omega_3)$, the complex refractive index of the nonlinear medium at the ir frequency.

We can show that, in a zone of large dispersion of the linear response of the medium, the $\vec{k}_T$ wave is an inhomogeneous wave. In order to show that it is convenient to express $\cos\varphi'_T$ in the form $\cos\varphi'_T = pe^{i\psi}$. Expressions for p and ψ in terms of the relative (scalar) phase mismatch $\Delta = (n_s - n'_T(\omega_3))/n'_T(\omega_3)$ and of the relative absorption parameter $\delta = n''_T(\omega_3)/n'_T(\omega_3)$ of the nonlinear medium are immediately obtained from the generalized Snell equations given above:

$$p^2\cos 2\psi = 1 - (1+\Delta)^2\,\frac{1-\delta^2}{(1+\delta^2)^2}\,\sin^2\varphi'_s\,,$$
$$p^2\sin 2\psi = \frac{2\delta(1+\Delta)^2}{(1+\delta^2)^2}\,\sin^2\varphi'_s\,. \quad (27)$$

Furthermore, the spatial argument of the $\vec{k}_T$ wave, $\vec{k}_T\cdot\vec{r}$, may be written in the following form:

$$\vec{k}_T\cdot\vec{r} = k_T(x\sin\varphi'_T + z\cos\varphi'_T) = k'_T\{x(1+\Delta)\sin\varphi'_s + zp[(\cos\psi - \delta\sin\psi) + i(\sin\psi + \delta\cos\psi)]\}\,, \quad (28)$$

x and z being the spatial coordinates corresponding, respectively, to the x axis, belonging to the incidence plane and to the boundary plane, and to the z axis.

We verify that the surfaces of constant amplitude of the $\vec{k}_T$ wave are given by $z = \text{const}$ and are therefore planes parallel to the boundary. The surfaces of constant real phase are given by $x(1+\Delta)\sin\varphi'_s + zp(\cos\psi - \delta\sin\psi) = \text{const}$ and are planes whose normals make an angle φ''_T with the z axis where

$$\cos\varphi''_T = \frac{p(\cos\psi - \delta\sin\psi)}{[(1+\Delta)^2\sin^2\varphi'_s + p^2(\cos\psi - \delta\sin\psi)^2]^{1/2}} \simeq (1 - \Delta\tan^2\varphi'_s)\cos\varphi'_s\,,$$
$$\sin\varphi''_T = \frac{(1+\Delta)\sin\varphi'_s}{[(1+\Delta)^2\sin^2\varphi'_s + p^2(\cos\psi - \delta\sin\psi)^2]^{1/2}} \simeq (1+\Delta)\sin\varphi'_s\,. \quad (29)$$

The simplified expressions appearing in Eq. (29) correspond to assuming $\Delta \ll 1$, $\delta \ll 1$, and $\Delta\tan^2\varphi'_s \ll 1$. With these approximations the planes of equal amplitude are still given by $z = \text{const}$ and the direction of the normal to the constant-phase planes is determined by Δ and not by δ. However δ is still responsible for the inhomogeneous character of the wave, owing to Eq. (27). The following simplified expression for $\vec{k}_T\cdot\vec{r}$ holds:

$$\vec{k}_T\cdot\vec{r} \simeq k'_T[x(1+\Delta)\sin\varphi'_s + z\cos\varphi'_s(1 - \Delta\tan^2\varphi'_s) + iz\delta/\cos\varphi'_s]\,. \quad (30)$$

To our knowledge, the inhomogeneous character of the propagation equation has not been considered in detail by previous works dealing with nonlinear optical parametric processes.

In the present theory the linear behavior of the

medium is taken into account by the refractive index $n'_T(\omega)$ and by the absorption parameter $\delta(\omega)$. Assuming the Lorentz oscillators model for the lattice,[24] these quantities may be written in terms of the well-known Huang dispersion relations[27] $n'_T(\omega) = \{\mathrm{Re}[\epsilon_\infty + \omega_p^2/D]\}^{1/2}$ and $\delta(\omega) = [n'_T(\omega)]^{-1}\{\mathrm{Im}(\omega_p^2/D)\}^{1/2}$. They exhibit a resonant behavior for $\omega \simeq \omega_0$ that affects in different ways the amplitude and the phase of the reflected field $\vec{E}_R$ and of the transmitted field $\vec{E}_T$.

The intensities of the $\vec{k}_R$ and $\vec{k}_T$ fields are found by writing the continuity equations for the electric and magnetic fields at the boundaries. Furthermore, the continuity condition for the transverse components of the momenta, expressed by the generalized Snell equation given above, leads to the condition of real propagation of the fields.

For the reflected field that condition is $\sin\varphi'_R \ll 1$, leading to the following one: $\sin\varphi'_s \leq [n'_T(\omega)(1+\Delta)]^{-1}$. The amplitude of that wave is found to be[40]

$$E_R = \frac{[d'_E + d'_Q(\omega_p^2/D)]}{\epsilon_s - \epsilon_T} \frac{n_s\cos\varphi'_s - n_T\cos\varphi'_T}{n\cos\varphi'_R + n_T\cos\varphi'_T} |E_1E_2^*| . \tag{31}$$

In the vicinity of the reststrahl band the condition of real propagation for the $\vec{k}_R$ field leads us to consider only very small angles φ'_s, φ'_R, φ'_T. For normal reflection and for Δ, δ, and (n/n'_T) much smaller than 1, the amplitude of the reflected field may be written in a simple and significant way:

$$E_R \simeq \frac{d'_E|E_1E_2^*|}{2\epsilon_\infty} \frac{D + C\omega_0^2}{D + \beta\omega_0^2} , \tag{32}$$

where $\beta = \omega_p^2/(\omega_0^2\epsilon_\infty) = S/\epsilon_\infty$, and $C = S(d'_Q/d'_E)$ is the nonlinear parameter we have defined in Sec. II. We verify that, with the given approximations, the reflected field is proportional to the ratio of the nonlinear contribution to the dielectric constant at frequency ω_3 and of the same (linear) dielectric constant. A measurement of the intensity and of the phase of the nonlinearly reflected wave as a function of ω_3 would lead to a direct measurement of the parameter $C(\omega_3)$ that characterizes the nonlinear response of the crystal. By introducing the field $E_s = [d'_E(1 + C\omega_0^2/D)/(\epsilon_s - \epsilon_T)]|E_1E_2^*|$, a nonlinear reflectivity $R = (|E_R|^2/|E_s|^2)$ can be defined that is formally identical to the usual expression of the linear reflectivity of linear optics[41] provided we reinterpret, in an obvious way, the quantities n_s and φ'_s appearing in Eq. (31). The simple expression (32) obviously does not hold for ω_3 lying in the reststrahl band in which $\Delta \gg 1$. It must be replaced by a more involved and less transparent expression. Of course, as far as nonlinear reflectivity is concerned, the reststrahl band keeps in the nonlinear regime most of its well-known linear properties. Optical propagation in the reststrahl band will be considered in Sec. IV.

The wave traveling into the nonlinear medium comes from the interference of the solution $\vec{E}_s$ given by Eq. (26) with the transmitted (inhomogeneous) wave $\vec{E}_T$ which is the solution of the homogeneous propagation equation (23). In the case in which the nonlinear polarization is orthogonal to the incidence plane defined by $\vec{k}_1$ and $\vec{k}_2$ and for $\Delta \ll 1$, we are led to the complete solution of Eq. (23) through the continuity equations for the electric and magnetic fields at the boundary. Writing the transmitted wave in form of a plane wave, the complete solution may be given in the following form:

$$\vec{E}_q(\omega) = \frac{\vec{p}d'_E(1 + C\omega_0^2/D)|E_1E_2^*|}{2n'_T(\Delta + i\delta)} e^{i\vec{k}_s\cdot\vec{r}} \times\{1 - A_T\exp[-k'_T(\delta + i\Delta)(z/\cos\varphi'_s)]\} , \tag{33}$$

where[40]

$$A_T = \frac{n\cos\varphi'_R + n_s\cos\varphi'_s}{n\cos\varphi'_R + n_T\cos\varphi'_T} \simeq \frac{n_s + n - [n_s^2/(2n)]\sin^2\varphi'_s}{n_T + n - [n_s^2/(2n)]\sin^2\varphi'_s} . \tag{34}$$

Equations (33) and (34) correspond to the condition $|\varphi'_s| \ll (\pi/2)$.

We can verify in Eq. (33) that the surfaces of constant amplitude of the wave $\vec{E}_q$ are planes parallel to the boundary.[40] We can also verify that the phase-matching parameter $\Delta \ll 1$, which affects in a quasiresonant way the undamped transmitted wave[8], appears in the exponential argument of the free solution and in the expression of A_T. The approximate expression of A_T given in (34), valid for φ'_s small, may be further simplified by setting $\varphi'_s = 0$, $n = 1$, $\delta \ll 1$, $\Delta \simeq 0$. It reduces in that case to the simple equation $A_T \simeq (1 - i\delta)$, which corresponds to the simplified expression of $\vec{E}_R$ given in (32).

As we have remarked in Sec. II, it is interesting to take into consideration the particular wave solution $\vec{E}_s$ of the propagation equation because, in the approximation that neglects parametric gain effects and for an interaction length L much larger than $(k''_T)^{-1}$, it gives the amplitude of the ir wave generated in the crystal. We can verify in Eq. (33) that in the range of polariton frequencies in which phase matching of the interaction can be achieved and for $\delta \ll 1$, the driven wave intensity F_s^2 is a Lorentzian function of Δ if k''_T is independent of k'_T. This behavior has recently suggested to us (cf. Ref. 8) making use of the coherent excitation of the polaritons as a useful means in studying the optical linear and nonlinear response of the crystal near the reststrahl band: A zone in which the large optical absorption of the medium does not allow in practice accurate measurements of the optical parameters by the usual methods of the linear spectroscopy of solids.[44,45] On the basis of that particular application of the method of coherent excitation, in Ref. 8 is also

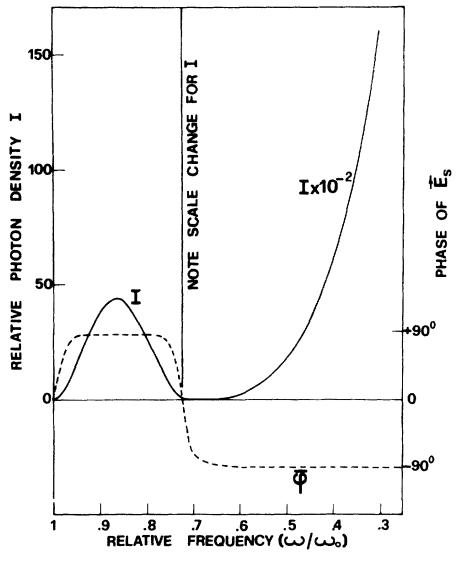

FIG. 3. Frequency dependence of the photon density $I = |\beta\epsilon_\infty/d'_E E_1 E_2^*|^2$ and of the phase $\bar{\varphi}$ of the ir field. The curve is drawn for GaP ($\omega_0 \simeq 366$ cm^{-1}).

proposed a general method of nonlinear spectroscopy (spectroscopy in the *momentum space*) which should be of great interest for the study of the optically active elementary excitations in solids which exhibit a large group velocity.[8,46] In our present experiment as well as in that described in Ref. 8, the large absorption at the idler frequency ω_3 and the practical absence of parametric gain are most useful effects, for the following reasons:

(a) The intensity of the ir field generated in the crystal is independent of z for $z \gtrsim (k''_T)^{-1}$. Consequently the emitted intensity that carries information on the crystal parameters to be measured is independent of the crystal thickness L if L is shorter than the coherence length of the mixing interaction. We note that the indirect measurement of the nonlinear optical parameters through the determination of the gain of a stimulated parametric process, as is usually done in nonlinear optics,[12] involves in general very critical experiments and a large uncertainty as to the results.

(b) The measurement of the physical parameters under investigation (e.g., the ir absorption coefficients and the nonlinear optical susceptibility near the lattice resonance) is not affected, in our experiment, by surface effects because, in the less favorable experimental conditions, the amplitude of the field, E_q, is nearly zero at the entrance surface of the medium and small in the absorption layer. Consequently the quantities measured in our experiment always correspond to the behavior of the bulk of the crystal regardless of the large absorption of the reststrahl band. This consideration demonstrates the interest of the present "transmission" methods against the reflection methods of the linear and nonlinear optical spectroscopy of solids in a zone of large optical absorption.[45] Obviously the above considerations refer to a behavior of the parametric mixing processes which is quite general in nonlinear optics: They also apply to similar experiments involving elementary excitations other than optical phonons, such as acoustic phonons, magnons, plasmons, etc.

In case of perfect phase matching $\Delta = 0$, the amplitude of the driven solution appearing in Eq. (33) may also be written in the following simple form:

$$E_s = i \frac{d'_E |E_1 E_2^*|}{\epsilon_\infty \beta \Gamma \omega_3 \omega_0^2} D^* (D + C\omega_0^2) , \tag{35}$$

where $\beta = (S/\epsilon_\infty)$.

In Fig. 3 the relative intensity and the phase of the E_s field are plotted vs frequency for $\omega < \omega_0$, assuming a frequency-independent damping parameter Γ. As for Fig. 2, the values of the optical parameters corresponding to the plots of Fig. 3 are those of gallium phosphide. We have used the linear data reported by Barker[44] and we have adopted the value of C we have measured in the present experiment (cf. Sec. VII). By comparing Figs. 2 and 3, we can note the difference existing between the frequency distribution of the polariton density and the one of the corresponding photon density. That difference reflects the general definition of the polariton as a linear superposition of phonon and photon particles.[7,27] We notice that, unlike the frequency dependence of $\bar{\rho}_q(\omega)$, the one of E_s^2, viz., the photon density, shows a maximum in the frequency region located between the transverse optical phonon frequency ω_0 and the frequency $\tilde{\omega} = \omega_0(1 + C)^{1/2}$ which we have defined at the end of Sec. II. We notice that at $\omega = \omega_0$ and $\omega = \tilde{\omega}$ the phase $\bar{\varphi}$ of $\vec{E}_s$ shows a rapid change, keeping nearly constant elsewhere.

We have discussed so far the propagation of the general solution of the Maxwell equation for the ir field disregarding the final process of the emission of that field out of the crystal. The study of this process does not present particular complications. We limit ourselves to consider only the polarization wave generated by the two interacting optical fields in their first passage through the medium, disregarding secondary nonlinear processes arising after (normal or total) reflection of these beams at the exit boundary. In that case, we must consider separately the refraction of the free (damped) contribution to the ir field generated at the entrance boundary and the field E_s which is directly associated with the driven nonlinear polarization wave.

As far as the free solution is concerned, the usual Fresnel refraction theory applies without modifications.[41] The same theory is nevertheless no more valid in general for the driven solution and it must be substituted by the more involved analysis we

have previously adopted in connection with the nonlinear refraction at the entrance boundary. Thus, we are led to consider, in correspondence with the driven solution $\vec{E}_s$ at the exit boundary, a wave $\vec{E}_{ir}$ that is transmitted out of the crystal and a damped inhomogeneous wave reflected back in the medium. In conclusion, the em field, which is created in the crystal slab in a single pass interaction, comes from the interference of a undamped driven wave with wave vector k_s and two (propagating or evanescent) inhomogeneous waves originating at the boundaries and traveling in the crystal with wave vectors having moduli equal to $n'_T(\omega_3/c)$.

The direction of propagation of the transmitted ir field $E_{ir}(\omega)$ is still given by a set of generalized Snell equations analogous to the ones written for the entrance boundary. In addition, analogous considerations on the continuity at the boundary of the electric and magnetic fields lead to the amplitude of the refracted fields. We limit ourselves to give here, for sake of completeness, the expression of the field $|\vec{E}_{ir}(\omega)|$ that is radiated in a linear medium of refractive index n in a direction making an angle φ with the normal $\vec{z}'$ to the exit boundary:

$$E_{ir}(\omega) = E_s(\omega)\frac{n_s\cos\varphi_s + n_T\cos\varphi_T}{n\cos\varphi + n_T\cos\varphi_T} . \qquad (36)$$

In analogy with our previous discussion, φ_s and φ_T are the angles [lying in the range $(-\pi/2)/(\pi/2)$] made by the wave vectors of the corresponding beams, with $\vec{z}'$.

We have assumed so far that the phase matching of the difference-frequency three-wave interaction can be achieved throughout the polariton region. Actually in that region phase matching is a critical effect which can be achieved only in special conditions. Owing to our present interest in cubic crystals, we shall limit ourselves to discussing briefly the process of "dispersion" phase matching which is based on the combined effects of the optical dispersion affecting the optical frequencies ω_1 and ω_2 and the near-resonance ir frequency $\omega_3 = (\omega_1 - \omega_2)$. This process, which to our knowledge has been first applied by Henry and Hopfield,[13] is very different from the widely used phase-matching effect that relies on the optical anisotropy of the medium[47,48] and that does not apply to cubic crystals.

The consideration of the kinematics of our interaction in an isotropic (cubic) crystal leads to the following condition for phase matching: $|k_1 - k_2| \leq k_3 \leq k_1 + k_2$ being $\omega_1 - \omega_2 = \omega_3$. That condition can be met in practice if the value of the refraction index n at the optical wavelengths $\lambda_1 = (c/\omega_1)$ and $\lambda_2 = (c/\omega_2)$, and of $(\partial n/\partial\lambda)_{\lambda\simeq\lambda_1}$ are sufficiently large, e.g., owing to the optical dispersion near the edge of the band gap of a semiconductor. If the optical beams are traveling in the same direction, the condition of collinear phase matching is given by the following equation, valid for $\omega_3 \ll \omega_1 \sim \omega_2$:

$$n_s \equiv \left[n(\lambda_1) - \left(\frac{\partial n}{\partial\lambda}\right)_{\lambda=\lambda_1}\left(\frac{\lambda_1}{\lambda_2}\right)\lambda_1\right] = n'_T(\omega_3) . \qquad (37)$$

Equation (37) can be simplified by setting $(\lambda_1/\lambda_2) = 1$. Condition (37) is actually verified in many cubic crystals over an extended range of ir frequencies lying in the lower branch of the polariton dispersion curve, if ω_1 and ω_2 lie in a zone of normal optical dispersion of the crystal. Dispersion phase matching in the upper branch of the polariton dispersion curve or in the reststrahl band implies one or both optical frequencies lying in a zone of anomalous dispersion of the crystal, e.g., near a strong exciton or impurity resonance.

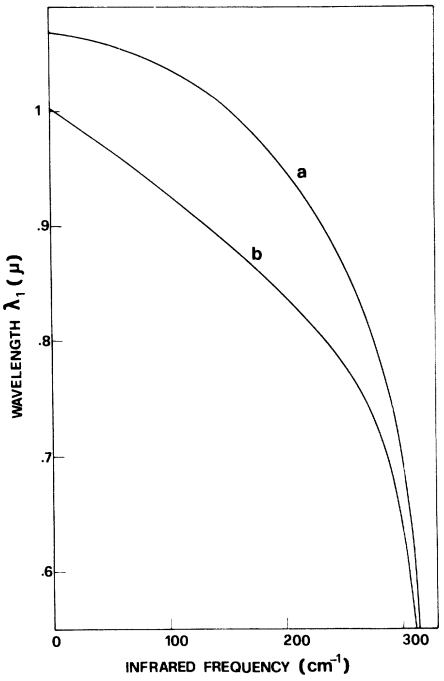

FIG. 4. Plots of the optical wavelength λ_1 vs infrared frequency satisfying to the condition of collinear phase matching in GaP. Curve (a) has been drawn on the basis of the single-oscillator model for the lattice, while curve (b) corresponds to the three-oscillator model (see text).

In Fig. 4 the optical wavelength λ_1 that satisfies Eq. (37) is plotted vs the corresponding ir frequency ω for gallium phosphide. In drawing curve (a) of Fig. 4 we have used the ir data reported by Kleinman and Spitzer[49] and extrapolated to low ir frequency, making use of the Lorentz single-oscillator model for the lattice resonance.[24] Curve (b) corresponds to the correction to the above data proposed by the theoretical work of Barker[44] on the basis of a multiple-oscillator model for the lattice in GaP. Furthermore, in Fig. 4 we have made use of the data for the index of refraction at optical frequencies reported by Nelson and Turner,[50]

Bond,[51] and Welcher.[52] We have observed that the optical data reported by these authors are in very good reciprocal agreement and therefore we take them confidently as the basis of the interpretation of our experimental results. We notice that the condition of collinear phase matching corresponding to Fig. 4 is very critically dependent on $n'_T(\omega_3)$, viz., on the model used for the lattice, and therefore the experimental check of the phase matching, even only at one ir frequency, can give a useful information on the dispersive behavior of the crystal in the ir. In addition, Fig. 4 shows that collinear phase matching in GaP is possible for generation of ir frequencies ranging from zero to about 300 cm^{-1}, this limit corresponding to the shortest wavelength transmitted through the crystal ($\lambda_{gap} \simeq 0.65\,\mu$). The excitation of polaritons with frequencies up to $\omega_0 \simeq 366$ cm^{-1} is possible using a noncollinear phase-matching configuration.[8]

IV. ir GENERATION IN THE RESTSTRAHL BAND

In linear optics the most striking properties of the reststrahl band concern the reflection and the transmission of the em radiation through the crystal.[24] It seems interesting, therefore, to consider briefly in the present section the intensity of the nonlinearly reflected and emitted fields $\vec{E}_R(\omega_3)$ and $\vec{E}_{1r}(\omega_3)$ when $\omega_3 = \omega_1 - \omega_2$ lies in the reststrahl band.

In the reststrahl band the phase matching of our three-wave interaction, i.e., the resonant nonlinear creation of a coherent polariton field, is possible only in very special cases. If ω_3 lies in the zone of anomalous ir dispersion, viz., $0 \leq \omega_3 - \omega_0 \lesssim \Gamma$, the phase-matching condition can be achieved with ω_1 and ω_2 lying in a zone of normal optical dispersion. In that case we should consider that, for $\omega_3 \approx \omega_0$, the absorption coefficient of the crystal is very large and therefore $E_s(\omega_3)$ becomes negligible, as shown in Fig. 3. Conversely, for normal dispersion in the infrared, viz., $\omega_0 + \Gamma \lesssim \omega_3 \leq \omega_{LO}$, it must be $n_s \simeq 0$, i.e., one or both optical frequencies must lie in a zone of anomalous dispersion of the medium, owing to Eq. (37).

We assume here a non-phase-matched configuration in which the two optical beams are striking the crystal in a direction normal to the entrance boundary. The free solutions of the Maxwell equation, Eq. (23), arising at the boundaries and traveling in the medium, are heavily damped (or evanescent) waves while the nonlinearly driven polarization wave at frequency ω_3 and the associated field $\vec{E}_s(\omega_3)$ propagate in the crystal without damping, with wave vector $\vec{k}_s = \vec{k}_1 - \vec{k}_2$. In addition, at the entrance and exit boundaries of the crystal, the nonlinear polarization gives rise, respectively, to a reflected field $\vec{E}_R(\omega_3)$ and to a transmitted one $\vec{E}_{1r}(\omega_3)$ which are emitted in the linear medium in the directions that are prescribed by the generalized Snell equations discussed in Sec. III.

By assuming the approximation of zero damping, $\Gamma \simeq 0$, the linear dielectric constant ϵ'_T as well as the nonlinear optical susceptibility d exhibit a sharp discontinuity at $\omega_3 = \omega_0$. Furthermore, the refractive index of the crystal is a pure imaginary throughout the reststrahl band and it is given by the expression $n_T = i\,|\epsilon'_T|^{1/2} = i\,[(S\omega_0^2/|D'|) - \epsilon_\infty]^{1/2}$.

The intensity of the nonlinearly reflected field at the entrance boundary of the crystal and emitted in the linear medium with refractive index $n = 1$ is given by the following expression, corresponding to Eq. (31):

$$|E_R(\omega_3)|^2 = \frac{d'^2_E [D' + C\omega_0^2]^2 |E_1 E_2^*|^2}{\epsilon_\infty^2 [D'(1-\xi^2) + \beta\omega_0^2][D'(1-\zeta^2) + \beta\omega_0^2]}, \tag{38}$$

where $\xi^2 = n_s^2/\epsilon_\infty$ and $\zeta^2 = 1/\epsilon_\infty$. It is easy to prove, owing to Eqs. (26) and (36), that the intensity of the transmitted field $\vec{E}_{1r}(\omega_3)$ is given by an expression that is identical to Eq. (38). We notice that, setting $\epsilon_\infty \gg 1$ and $\zeta = 0$ in Eq. (38), $E_R(\omega_3)$ and $E_{1r}(\omega_3)$ rise rapidly toward an infinite value for ω_3, approaching the frequency of the longitudinal optical mode $\omega_{LO} = \omega_0(1+\beta)^{1/2}$. A similar behavior is not shown by the reststrahl reflectivity or transmissivity in the linear regime.[45] Of course, a more accurate analysis that accounts for the complete complex expressions of ϵ_T and of d would find that the damping prevents E_R and E_{1r} to become infinite at $\omega_3 = \omega_{LO}$.

We do not further develop here the theory of the ir generation in the reststrahl band as polaritons are not largely involved in the dynamics of a highly non-phase-matched process.

We postpone a detailed description of this interesting process to a later paper.

V. EXPERIMENTAL APPARATUS

The experimental arrangement of our work (Fig. 5) was partially similar to the one of an experiment of coherent excitation of polaritons, detected by an up-conversion scattering technique we have recently reported.[8] The ruby laser was Q switched by the combined effects of a cryptocyanine saturable dye cell and a rotating prism, and it worked on a single axial mode with a linewidth of ~ 0.01 cm^{-1}. The laser pulse duration was ~ 20 nsec and the beam divergence was $\sim 8\times10^{-4}$. The output beam of the laser, having a diameter of about 10 mm, was split by an adjustable 90° prism mounted externally to the cavity and totally reflecting on a path orthogonal to the axis of the laser, about half of the transverse section of the laser beam.

Two Raman liquid cells, 9 cm long, were inserted in the paths of the two beams in order to generate two coherent Stokes waves at the frequencies ω_1

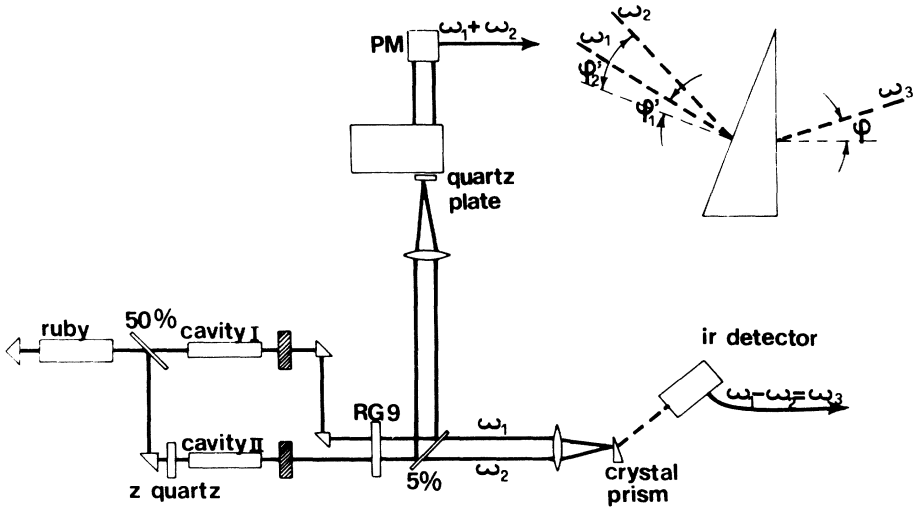

FIG. 5. Schematic diagram of the experimental apparatus.

and ω_2.

In such configuration the Raman cavities were terminated by dielectric coated front mirrors and, in the back side, by the laser Fabry-Perot. Care was taken to avoid superposition in the laser of the Stokes frequencies by properly mounting the beam splitting prism. That splitting device, one of the most critical parts of our arrangement, was made to intersect the laser beam in an adjustable way in order to allow for a proper balancing of the emitted Stokes waves. We have represented in Fig. 5 the beam splitting prism as a 50% splitter plate. Besides the external insertion of the Raman cavities in the system, we have tried succesfully to excite directly the stimulated Raman (SR) effect in the laser Fabry-Perot. In that configuration the laser was constituted by two independent noninterfering ruby + Raman oscillators terminated in the front side by two wide-band dielectric coated mirrors and, in the back side, by the common Q-switching rotating prism. The position of the beam splitting prism determined the transverse sections of the ruby rod (diam = 10 mm) that were made active in either oscillators. In the two configurations we have just described, the amount of the Stokes energy emerging from the wrong arm of the complex cavity never exceeded 5% of the total Stokes generated at that frequency. The direct insertion of the Raman cells in the laser Fabry-Perot (FP) was found to give the best results with respect to the frequency purity of the Stokes waves. However it gave also the most critical configuration with respect with the simultaneous oscillation of the two cavities, and a good balancing of the output Stokes intensities was possible only with active liquids of comparable SR efficiency: a critical condition to meet. Other possible arrangements (mixing of two liquids in a single cell, aligning two cells on the same path) were tried with some success but they are not advisable in general because, in general, they do not allow a flexible balancing of the output Stokes intensities.

With the laser working at a relatively low pump power (peak power ~ 3 MW at 6943 Å) the Raman linewidths did not exceed 1 cm^{-1} when only a single mode of the laser radiation was present. At the output of the Raman cavities a Schott RG 9 glass filtered out the 6943-Å radiation. A small fraction of the Stokes beams, deviated by a 5% beam splitter, was focused by a 10-cm-focal-length lens on an x-cut quartz plate, 150 μ thick, that was mounted in front and very near to the entrance slit of a Hilger-Watts 292 grating spectrometer. At the output of the spectrometer the non-phase-matched uv radiation at the sum frequency $\omega_1+\omega_2$ was detected by a 56 UVP photomultiplier and it provided the reference signal for our difference-frequency mixing experiment.

We could easily assume that the nonlinear response of quartz is substantially frequency independent in the 3000–4000-Å wavelength range provided the strong frequency dependence of the coherence length[12]

$$l_{\mathrm{coh}} \simeq (2\pi c/\omega_1)(n_{2\omega_1} - n_{\omega_1})^{-1}$$

is compensated for. In order to solve this problem the output surface of the quartz plate was ground with emery powder with grain size of the order of l_{coh}. As l_{coh} is of the order of several microns in the optical range in quartz (in our case $l_{\mathrm{coh}} \simeq 8$ μ) even a very narrow beam (e.g., in the focal region of a 10-cm focal-length lens) is testing, upon transmission through the crystal and over its transverse section, a large set of effective interaction lengths differing among themselves by fractions of l_{coh}. Consequently the frequency dependence of the output

sum-frequency intensity is statistically cancelled out over a large range of the frequencies ω_1 and ω_2. The scattering effects arising at the ground face of the crystal were easily prevented by simply sticking the quartz plate to a thin glass plate with silicone oil. The compound plate so obtained exhibited a perfect transparency and no appreciable light scattering was detected upon transmission through it of an Ar laser beam. We believe that the simple technique we have just described could be of substantial interest for similar applications in nonlinear optical experiments in which the lack of phase-matching causes unwanted effects of frequency dispersion of the emitted intensity. The auxiliary spectroscopic arrangement we have just described was also used during the experiment for measuring the linewidths of the Raman waves and for checking the absence of spurious broadening effects in the Raman liquids due to self-steepening or self-phase-modulation processes.[53]

The two Stokes beams, with frequencies ω_1 and ω_2, having a divergence $\simeq 3\times10^{-3}$ were focused by a common high-quality lens on a gallium phosphide crystal in which a coherent polariton field at the different frequency $\omega_3 = \omega_1 - \omega_2$ and wave vector $\vec{k}_T = \vec{k}'_T + i\vec{k}''_T$ was generated. The angle ϑ made by the mean directions of the Stokes wave vectors $\vec{k}_1$ and $\vec{k}_2$ in the crystal was set to a previously calculated value in order to secure the phase matching of the process, as will be discussed in Sec. VI. Changes of the polarization of the beams were made possible by the insertion of z-cut quartz plates of proper thickness in the optical paths of the Stokes beams. The GaP crystal was mounted at the center of an adjustable goniometer having a common rotation axis with a second independently adjustable goniometer holding the ir detector on its arm.

The ir detector we used was a triglycine sulphate (TGS) pyroelectric detector[54,55] working at a temperature near to the ferroelectric Curie point of TGS ($\simeq 49\,^{\circ}$C).[56] The detector has been designed for our experiment at the Laboratoire de Spectroscopie Infrarouge of the University of Nancy (France). In designing the detector it has been chosen the configuration in which the active surface contains the pyroelectric c axis. That configuration corresponds to the same limit value of the signal-to-noise ratio as for the c axis perpendicular to the active surface[55] but it has the advantage that the signal is enhanced of the ratio l/d between the length l of the TGS plate in the direction of the c axis and the thickness d of the plate. In our case we had $l = 4$ mm and $d = 200$ μ. One disadvantage of the configuration we used is that the absorption of the ir radiation must be provided by the TGS plate itself. However, if one chooses the proper orientation of the crystal with respect to the polarization of the ir wave, a complete absorption of the incoming radiation in the wavelength range (5–100 μ) is compatible with very small values of d and of the thermal response time of the detector owing to the very large infrared absorption of the TGS crystal.[55] In the range of ir frequencies at which the detector was operating in our experiment (300–400 cm^{-1}) the absorption coefficient of TGS has been found to be a slowly decreasing function of frequency with an average value about equal to 800 cm^{-1} [55] (c axis parallel to the E_{1r} field). The signal generated across the pyroelectric crystal was preamplified by a first stage of gain 40 having an input resistance matched to the equivalent resistance of the crystal $\simeq 10^5$ Ω. It was further recorded by an oscilloscope CRT using a narrow-band high-gain Tektronix plug-in amplifier type E. A typical signal corresponding to a 1-μW, 20-nsec ir pulse emitted at $\lambda = 34.6$ μ is shown in Fig. 6. The rise time of the signal is ~ 8 μ sec and the signal-to-noise ratio is about 20. Working in the condition of high detectivity, as in our case, requires a large value of the resistance shunting the crystal and the observation of the actual shape of the generated ir pulse is obviously lost. However the amplitude of the corresponding integrated electric signal has been found to be proportional to the incident infrared power within 1% for a mean incident flux of 10^{-3} W/cm^2 at $\lambda = 34.6$ μ.[57] In spite of the slow response of the pyroelectric detector in the high detectivity configuration, it exhibits a sensitivity that is practically frequency, independent over a large range of radiation wavelengths in the infrared. Furthermore, the simple and inexpensive operation of this device may be largely appreciated when is involved in experiments carried out over an extended period of time, as in our case. Some inessential anomalies of the response of the detector related to piezoelectric shock effects[58] may be easily identified at the output and they can be prevented by avoiding radiation overloading of the active surface. To our knowledge, our present work reports the first application of the pyroelectric detector as an essential part of a physical experiment of nonlinear optics. This motivates the somewhat extended description we gave of our thermopile in order to

FIG. 6. Pyroelectric detector signal corresponding to the detection of a 1-μW 20-nsec ir pulse emitted at $\lambda = 34.6$ μ.

point out some experimental problems that could arise in the pyroelectric detection of ir nanosecond pulses in the μW range.

The calibration of the absolute sensitivity our ir detection system was performed by detecting one of the optical Stokes beams through a set of calibrated Wratten filters taking further into account the ratio of the absorption coefficients and of the reflectivity of TGS at $\lambda \simeq 30\ \mu$ and $\lambda \simeq 0.7\ \mu$.[55] The frequency of the infrared radiation generated in our difference-frequency generation experiment was first identified with an ir grating spectrometer but the bulk of the experiment was carried out by making use of an efficient set of filters composed by a 2-mm-thick Si plate, a 0.2-mm carbon polyethylene sheet and by a 4-mm-thick KRS-5 plate. These filters combined with the strong absorption of the reststrahl band of the GaP specimen were very effective in isolating the detector practically over the entire frequency spectrum against radiation arising from occasional sparks occurring at the front surface of the crystal. In order to avoid registration of spurious effects, the disappearance of the signals upon absence of one of the exciting Stokes beams was tested repeatedly during the experiment. We found in practice that, with the intensity of our laser beam, the spurious events were very rare.

VI. MEASUREMENT OF LINEAR OPTICAL PARAMETERS OF GaP

In a first experiment we studied the polariton excitation in GaP at an ir frequency $\omega_3 = 289\ \text{cm}^{-1}$ by beating two coherent beams with wavelengths $\lambda_1 = 7429$ Å and $\lambda_2 = 7273$ Å The Raman liquids excited in SR scattering in the two cavities were, respectively, C_6D_6 and CS_2.[59] This condition is of particular interest because, by calculating the values of k_1 and k_2 on the basis of the known optical data for GaP (Refs. 50–52 and Sec. III) and k'_T using the ir data reported by Kleinman and Spitzer[49] and extrapolated in the far ir using the Lorentz single-oscillator model for the lattice,[24] we should have found a perfectly collinear phase-matching condition for the interaction (i.e., $\vec{k}_1$ parallel to $\vec{k}_2$ and $\vec{k}'_T$). In fact, this condition was not verified in the experiment: When the distributions of the $\vec{k}_1$ and $\vec{k}_2$ vectors of the Stokes beams were spatially superimposed in the crystal with a divergence $\simeq 6\times10^{-3}$, we found that the polariton field was generated with a distribution of $\vec{k}'_T$ vectors lying about a small angle cone ($= 18°$ in the crystal). In order to avoid large incidence angles of the optical beams at the entrance face of the crystal and radiation trapping of the ir wave by total internal reflection at the exit face, we made use of a GaP prism cut at 19°. The two Stokes beams were focused by a high-quality ir achromatic 10 f/1 lens approximately in a direction orthogonal to the entrance face of the prism. Throughout the experiment we made the exit face of the crystal to coincide with the crystallographic (110) plane and the crystallographic z axis parallel to the prism edge and to the common rotation axes of the goniometers holding the prism and the detector (cf. Sec. V). Furthermore, the electric fields of the interacting optical waves, $\vec{E}_1$ and $\vec{E}_2$, were set orthogonal to the z axis. With that configuration the source polarization in the crystal is written in terms of the interacting fields as $P_z^{\text{NL}}(\omega_3) = d_{z,j,k}E_{1,j}(\omega_1)E^*_{2,k}(-\omega_2)$, $d_{z,j,k}$ being the z component of the nonlinear susceptibility tensor d.[12] For the crystal class $\bar{4}3m$, to which GaP belongs, d has nonzero and equal components only for all indices different.[33] In order to simplify the interpretation of our results, the crystal prism was rotated until the coherent ir beam was emitted in a mean direction orthogonal to the exit face.

The kinematical configuration of the collinear phase-matching condition at $\omega_3 = 289\ \text{cm}^{-1}$ corresponds to an ir wave vector k'_T equal to $1050\ \text{cm}^{-1}$, while the emission at an angle $\gamma = 18°$ with respect to $\vec{k}_1$, we have found in the experiment, corresponds to $k'_T = 1100\ \text{cm}^{-1}$ at the same frequency. This last figure corresponds to the following value of the refraction index of the crystal at $\lambda = 34.6\ \mu$ ($\omega_3 = 289\ \text{cm}^{-1}$): $n'_T = 3.819$. The large discrepancy of the two values of k'_T we have found has led us to the conclusion that the Lorentz single-oscillator model for the TO lattice oscillation is not valid in GaP and it must be replaced by a more refined model that accounts for strong multiple-phonon resonances at frequencies near to the fundamental TO frequency $\omega_0 = 366\ \text{cm}^{-1}$. These conclusions are substantiated by further experimental results to be reported in the present section and by an analogous kinematical discrepancy that has been found in the course of an experiment of near-zero-angle spontaneous scattering in GaP[13] and reported by Barker.[44] As will be clarified later in this section, spontaneous Raman scattering experiments, like the one reported in Ref. 13, suffer from an intrinsic lack of accuracy when they are applied to the measurement of optical parameters in the quasicollinear configuration (viz., in the near-zero-angle scattering) and in a frequency region of large optical dispersion of the crystal. Consequently they can hardly lead to more than qualitative conclusions on the behavior of the optical properties of the solid in that region. On the other hand, it is well known that spontaneous Raman scattering at large angles (e.g., at 90°) is a very useful and accurate tool for spectroscopic measurements in the vicinity of the fundamental frequency ω_0, where our present coherent method, and the one reported by us in Ref. 8, lack accuracy and cannot be conveniently applied. Therefore our coherent methods can be thought to be complementary to the usual methods of spontaneous spectroscopy

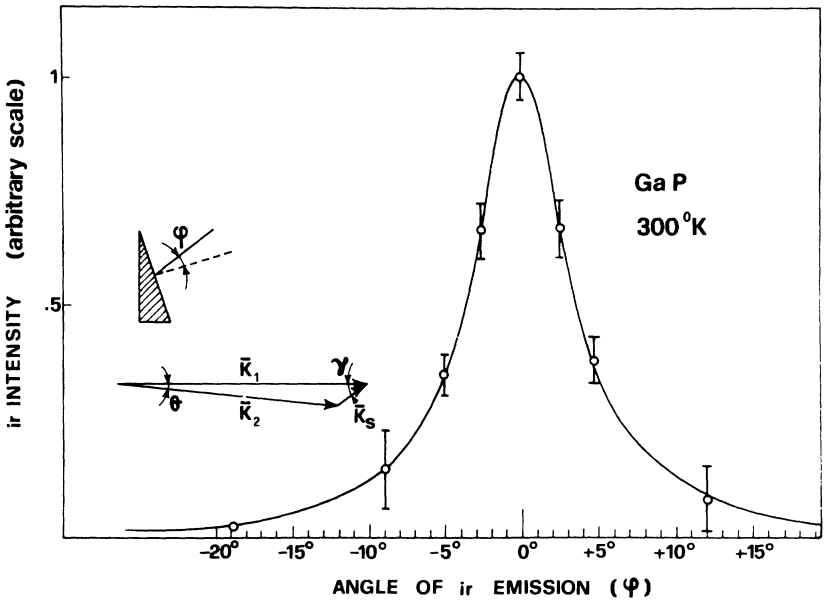

FIG. 7. Angular distribution of the ir intensity $I(\varphi)$ emitted at $\lambda = 34.6\ \mu$.

and give better results when the group velocity of the excitation under investigation is large (e.g., in a photonlike polariton zone).

The angular distribution of the emitted ir radiation $I(\varphi)$ in a plane orthogonal to the crystallographic z axis has been studied at $\omega_3 = 289\ \text{cm}^{-1}$ by rotating the goniometer arm holding the detector around the crystal at angles near to the angle of normal emission from the exit face $\varphi = 0$. The experimental values of $I(\varphi)$ are reported in Fig. 7. The resolution of our angular spectrometer was determined by the aperture of the sensitive surface of the detector and it was about equal to 2×10^{-2} rad. The shape of the curve reported in Fig. 7 is mainly determined by the dependence of the emitted ir intensity on the phase mismatch of the nonlinear interaction in the proximity of the condition of perfect phase matching in the crystal. The convergence $\bar{\delta}$ of the $\vec{k}_1$ and $\vec{k}_2$ beams in the medium ($\bar{\delta} \simeq 6\times10^{-3}$) made possible the excitation of the polariton field in a substantially large interval of mismatch angles centered on the phase-matching angle γ (see the sketch in Fig. 7). The theoretical expression of $I(\varphi)$ that has been used to draw the best-fit curve appearing in Fig. 7 may be given in the following form:

$$I(\varphi) = \frac{I_{ir}}{1 + [2\omega_3(\tan\gamma)/c\,\alpha(\omega_3)]^2 \sin^2\varphi} f(\gamma, \varphi) g(\gamma, \varphi_s, \vartheta)\ , \tag{39}$$

showing an Airy-functional dependence of $I(\varphi)$ on φ. In the above expression I_{ir} is the ir intensity emitted at zero angle $\varphi = 0$ in condition of phase matching and $f(\gamma, \varphi)$ is the modified Fresnel function accounting for the refraction of the $\vec{k}_s$ wave through the exit face of the crystal (see Ref. 40 and Sec. III). $g(\gamma, \varphi_s, \vartheta)$ takes into account the angular dependence of the components of the $\vec{E}_1$ and $\vec{E}_2$ vectors on the crystallographic directions x and y entering into the expression of the source polarization $P_z^{NL}(\omega_3)$. The angle ϑ is defined in the sketch of Fig. 7. We can verify that ϑ is very small in all the possible kinematical conditions corresponding to phase matching, owing to $k_1/k_T' \gg 1$. The explicit derivation of $I(\varphi)$ is given in Appendix B. The expressions of the functions f and g are found to be

$$f(\gamma, \varphi) = \frac{[2 + (\tan\gamma \sin\varphi)/n_T']^2 + \delta^2}{[1 + (\cos\varphi)/n_T']^2 + \delta^2}$$

and (40)

$$g(\gamma, \varphi_s, \vartheta) = \left\{\cos(2\varphi_s) \times \frac{(1 - \tan2\varphi_s \tan2\gamma) - \vartheta(\tan2\varphi_s + \tan2\gamma)}{1 - \vartheta\tan2\gamma}\right\}^2 .$$

The quantity δ is defined in Sec. III. We can easily verify that for small angles φ_s, i.e., $\varphi_s <$ (angle of total internal reflection), f and g are slowly varying functions of φ and of $\varphi_s \simeq (\sin\varphi)/n_T'$. We should notice in this connection than two further effects can reduce the angular resolution of our measurements. One effect is related to the effective linewidth of the exciting Stokes fields and the second effect is due to the angular divergence of these optical beams in the crystal. The former effect may be easily calculated by a simple geometrical argument (see Appendix B). If $\bar{\delta}$ is the linewidth of the Stokes radiation and $(\varphi_s)_{\bar{\delta}}$ is the value of the incidence angle φ_s when one of the exciting frequen-

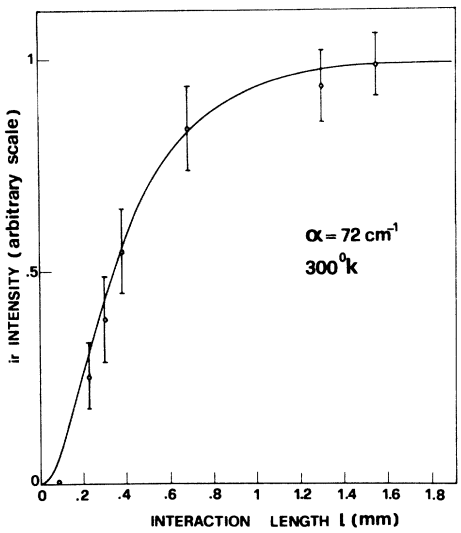

FIG. 8. Infrared intensity emitted at $\lambda = 34.6\ \mu$ in the phase-matching condition as a function of the interaction length l in GaP. The curve shows directly the spatial distribution of the em field in the crystal.

cies, say, ω_1, is perturbed by an amount $\frac{1}{2}\bar{\delta}$ about its mean value, we can write $\cos(\varphi_s)_{\bar{\delta}} - \cos(\varphi_s)_{\bar{\delta}=0} = \bar{\delta} k_1/(\omega_1 k'_T)$. In our case $\bar{\delta} = 1\ \mathrm{cm}^{-1}$ and $k_T = 1110$ cm at $\omega_3 = 289\ \mathrm{cm}^{-1}$. The corresponding value of $\Delta\varphi_s \equiv (\varphi_s)_{\bar{\delta}} - (\varphi_s)_{\bar{\delta}=0}$ is equal to $0.45°$ and, outside the crystal, $\Delta\varphi \simeq \Delta\varphi_s n'_T \simeq 1.7°$. The second effect is simply given by $\angle\varphi \simeq \bar{\bar{\delta}} n'_T$, where $\bar{\bar{\delta}}$ is the divergence of the optical beams in the crystal. In our case $\bar{\bar{\delta}} \simeq 6 \times 10^{-3}$, and we find $\Delta\varphi \simeq 1.1°$ at $\omega_3 = 289\ \mathrm{cm}^{-1}$. The maximum emitted ir intensity at $\omega_3 = 289\ \mathrm{cm}^{-1}$, $I(\varphi = 0) = I_{ir}$ was about 1 μW, while the power associated with the exciting Stokes pulses was ~ 5 kW (pulse duration 20 nsec). That experimental value of I_{ir} is eight times less than the one calculated on the basis of the value of the electro-optic coefficient of GaP by further taking into account the dispersion of the nonlinear optical susceptibility in the polariton region (see Refs. 25, 50 and 60 and Sec. VII). That discrepancy may be easily attributed to imperfect superposition of the interacting beams in the crystal and, possibly, to the lack of fulfillment of the critical condition, discussed in Sec. II, requiring that the coordinate $\bar{z}$ of maximum parametric transfer lies inside of our relatively thin crystal (in that experiment the interaction path was 2 mm).

In a further experiment the GaP prism, held on a micrometer mount fitted on the plate of the goniometer and kept oriented with the detector in the condition of phase matching $\varphi = 0$, was displaced in a direction parallel to the exit face and orthogonal to the goniometer axis, in order to vary the interaction length l of our parametric process. The results of the measurement of the ir intensity I_{ir} emitted as function of l are shown in Fig. 8, in which a best-fit theoretical curve $G(l)$, drawn on the basis of Eqs. (33), (34), and (36), is also reported.

We believe that the data reported in Figs. 7 and 8 give important and precise information on the linear optical parameters associated with the polariton dynamics in GaP. The determination of the angular position of the peak of the curve shown in Fig. 7 leads to a very sensitive measurement of the angle γ associated to the kinematics of the interaction, owing to the "amplifying" effect of the Snell law on the angles of light beams emerging from highly refractive materials (see Refs. 40 and 41 and Sec. III). As we have shown, the angle γ is strongly dependent on the modulus of the polariton wave vector $\vec{k}'_T$, particularly in the geometry of quasicollinear interaction. As a consequence, a precise determination of the ir index of refraction of the crystal over the entire polariton region is made possible by the present experiment. As we have shown at the end of Sec. III, that region may be extended down to zero frequency for the idler wave using appropriate sources of coherent radiation (e.g., tunable dye lasers). We can also note that the expressions (33) and (39) show a strong dependence of the shapes of both curves $I(\varphi)$ and $G(l)$ on the absorption coefficient $\alpha(\omega_s)$ of the crystal, suggesting two precise methods to measure that quantity. The curve $G(l)$ that fits best our data of Fig. 8 corresponds to a value $\alpha = 72(\pm 3)\ \mathrm{cm}^{-1}$ at $\omega_3 = 289\ \mathrm{cm}^{-1}$. That value agrees within 10% with the corresponding information given by the curve $I(\varphi)$ of Fig. 7. We should point out that the measurements of the absorption coefficient of crystals carried out by the conventional transmission methods [45,49] lose accuracy increasingly with α for $\alpha \gtrsim 50$–$60\ \mathrm{cm}^{-1}$ (see Ref. 44, Sec. III A, p. 165). Furthermore, the Kramers-Krönig analysis of the data obtained by the linear reflection methods in the vicinity of the lattice resonance where α is very large is an indirect method that often lacks accuracy. [45] In addition, the reflectivity data may be largely affected by surface effects mainly in highly anharmonic crystals in the vicinity of the lattice resonance. [45] Consequently, we believe that our present nonlinear transmission method that is not affected by surface effects should be of substantial interest in solid state spectroscopy.

The experiment on the angular distribution of the ir radiation has been carried out in conditions similar to the ones described above for two other polariton frequencies: $\omega_3 = 335\ \mathrm{cm}^{-1}$ ($\lambda = 29.9\ \mu$) and $\omega_3 = 342\ \mathrm{cm}^{-1}$ ($\lambda = 29.2\ \mu$). In these cases we made use of a GaP single-crystal prism cut at 40° and oriented as for the 19° prism. The former frequency was generated by beating the Stokes waves generated by the couple of Raman liquids C_6H_6-CS_2, while for the latter the liquids aniline-CS_2 were

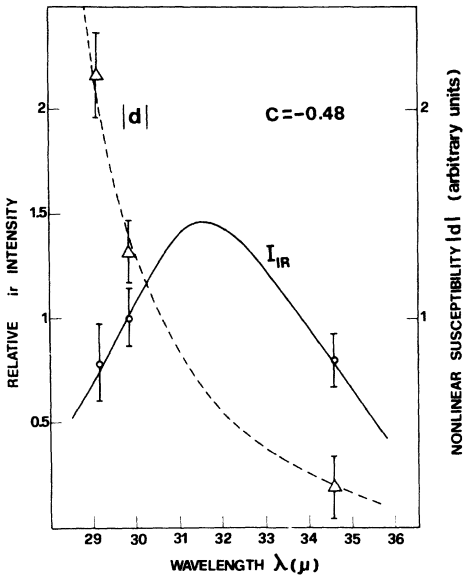

FIG. 9. Plot of the relative ir intensity vs λ arising from phase-matched processes at various wavelengths. The corresponding plot of the modulus of the nonlinear susceptibility $|d|$ of GaP is also given (arbitrary units).

used.[59] The values of n'_T and α at these frequencies were measured on the basis of the corresponding curves $I(\varphi)$. We found $n'_T = 4.77$, $\alpha = 450(\pm 20)$ cm^{-1} at $\lambda = 29.9\ \mu$, and $n'_T = 5.05$, $\alpha = 680\ (\pm 35)$ cm^{-1} at $\lambda = 29.2\ \mu$. The values of I_{ir} emitted at various wavelengths in the phase-matching condition at $\varphi = 0$ are reported in Fig. 9. As will be discussed in Sec. VII, the data of Fig. 9 lead to a measurement of the quantity $C = S(d'_Q/d'_E)$, a nonlinear property of GaP.[23]

The entire set of experiments was carried out successfully, but with large fluctuations of the results, using polycrystalline samples. Obviously, in that case, the interaction useful for ir generation took place only in the single crystals belonging to the layer immediately adjacent to the exit face of the specimen. The large scattering of the values of the emitted intensity is easily justified by the random orientation of these active crystals and by their random size.

As we have already remarked in this section and at the end of Sec. III, our present method is very sensitive in a zone of photonlike polaritons and it can lead to definite conclusions about the validity of a physical model that is assumed to describe the behavior of the crystal in the frequency zone under investigation. In the case of GaP an attempt at a realistic model for the optical phonon excitation may be found in the work[44] where a multiple-oscillator theory for the lattice is developed. We could verify that the results of our measurements are in fair agreement with the three-oscillator model discussed in Ref. 44 and therefore they establish, rather conclusively, the validity of that approximation. Finally, we want to remark in this connection that the accuracy of our results is mainly due to the high collimation of the coherent exciting beams. Owing to that, several linear and nonlinear effects of crystal optics could be used in order to measure the optical parameters. For instance, the values of the index of refraction n'_T were first measured with the method described in this section and were further doublechecked by measuring the angle at which the crystal prism must be rotated in order to observe the sharp extinction of the emitted radiation for total internal reflection at the exit face. We stress here that the same results could not be achieved with the same accuracy in a spontaneous scattering experiment owing to the intrinsic need for a substantially large aperture angle of the detection system. That is true in particular in a zone of large optical dispersion, as in the polariton region, where the near-zero-angle configuration critically requires a sharp definition of the scattered wave vector $\vec{k}'_T$.

VII. DISPERSION OF NONLINEAR OPTICAL SUSCEPTIBILITY OF GaP

The experimental values of the ir intensity I_{ir} emitted in the condition of phase matching $\varphi = 0$ at various wavelengths and reported in Fig. 9 lead to a direct evaluation of the relative values of the modulus of the nonlinear susceptibility $|d|$ owing to Eq. (26). If we assume here the validity of the simple single-oscillator model that was first adopted by Faust and Henry,[23] we can determine the value of the characteristic nonlinear quantity $C = S(d'_Q/d'_E)$ defined in Secs. II and III.[61]

The values of $|d|$ evaluated on the basis of the experimental values of I_{ir} are reported in Fig. 9 with the error flags calculated on the basis of the experimental uncertainties affecting the values of $I_{ir}(\lambda)$ as well as the ones of $n'_T(\lambda)$ and $\alpha(\lambda)$ measured in the present experiment. The best-fit curve $|d(\lambda)|$ calculated on the basis of the mentioned analytical expression of d corresponds to a value of $C = -0.48(\pm 0.01)$ that is about 9% larger than the one calculated on the basis of the Stokes intensities measured in LO and TO spontaneous Raman scattering[13] and reported in Ref. 23. Once the $|d(\lambda)|$ curve is drawn, we could plot the corresponding curve of $I_{ir}(\lambda)$ that fits our experimental points. We verify that the shape of the $I_{ir}(\lambda)$ curve is very similar to the corresponding curve of $|E_s|^2$ reported in Fig. 3. The only difference between the two curves is that the plot of Fig. 3 corresponds to a frequency dependence of n'_T and α as given by the single-oscillator theory, while in Fig. 9 we have made use of the experimental values of these quantities. That difference tends to become large at wavelengths far from the TO resonance owing to the increasing effect of the direct ir absorption

by combination phonon bands and local modes.[44] We can compare our experiment to the previous work of Faust and Henry[23] aimed at the study of the dispersion of $|d|$ near the reststrahl band in GaP. We believe that the up-conversion mixing method reported in Ref. 23 has one advantage over our method as it has been applied in the present work: It does not deal with a phase-matched interaction and consequently it can be applied over an extended range of ir frequencies including the region $\omega_3 > \omega_0$, where the dispersion phase matching is not allowed in cubic crystals (Cf. Sec. III). In addition, that method does not require adjustments of the direction of the beams and of the crystal orientation in order to secure phase matching. On the other hand, the non-phase-matching configuration requires a further data-reduction process on the results that must account for the different coherence lengths at various wavelengths.[12] That requires a previous knowledge of the values of the linear optical parameters $n_T'(\lambda)$ and $\alpha(\lambda)$ that must be taken for granted from the work of other authors or require an additional critical experiment. In our work linear parameters are directly measured on the specimen under investigation in the course of the same experiment. Furthermore, we should consider that working with relatively high-intensity pulses instead of cw low-power lasers avoids, in general, signal-to-noise problems in the detection that must be quite severe in a multiple-photon nonlinear experiment of this kind.

By comparing our results with the ones of the work of Ref. 23, we found a good agreement in the determination of C as the two measurements differ by about 3.5%. This result could be interpreted as a very good test of our method if one considers that it has been applied to only three values of ir wavelengths.

In conclusion, in Secs. VI and VII we have presented a new method of nonlinear spectroscopy that should be quite useful for the study of the optical properties of a large class of solids, in particular of the III-V semiconductors that have generally common dynamical properties in the linear as well as in the nonlinear regimes.[45] Furthermore, as far as GaP is concerned, in addition to the verification of a new nonlinear optical effect, we have reported new precise measurements of the optical parameters in the highly dispersive polariton region. In particular, our data of the absorption coefficient of GaP are the results of the first direct measurement of the quantity in that frequency region without recourse to that usual indirect Kramers-Krönig processing of the reflectivity data.[44]

ACKNOWLEDGMENTS

We wish to thank Professor J. Ducuing for very helpful discussions. We are also indebted to Professor A. Hadni of the University of Nancy and to Dr. H. Rodot of CNRS Laboratories, Bellevue, for the loan of ir equipment and for supplying large samples of GaP crystals.

APPENDIX A

The integration of the Hamiltonian density $\mathfrak{H}_i$ given by Eq. (4) is carried out over a volume V having linear dimensions much smaller than the inverse of the optical parameter that account for the most rapid spatial variation of the fields, e.g., the absorption coefficient α, in our case. As a consequence it involves, to a large approximation, only the complex exponential terms appearing in (4).

Let us calculate the integral over a cube of volume V:

$$\int_V \exp(i\Delta\vec{k}\cdot\vec{r})\,dV = \frac{V}{\bar{x}}\int_0^{\bar{x}} \exp[(i\Delta k' - \tfrac{1}{2}\alpha)\,x]\,dx\,, \tag{A1}$$

having taken one of the cube edges, of length $\bar{x}$, parallel to $\Delta\vec{k}$. The integrand on the right-hand side of (A1) may be written in terms of circular functions and the corresponding integral may be reduced to the complex sum of the two sine and cosine Fourier transforms $S_{\Delta k}\{F(x)\}$ and $C_{\Delta k}\{F(x)\}$ of the function $F(x) = \exp(-\frac{1}{2}\alpha x)$ in the $\Delta k'$ space:

$$\int_0^{\bar{x}} \exp[(i\Delta k' - \tfrac{1}{2}\alpha)\,x]\,dx = \int_0^{\bar{x}} \cos(\Delta k' x)\exp(-\tfrac{1}{2}\alpha x)\,dx + \int_0^{\bar{x}} \sin(\Delta k' x)\exp(-\tfrac{1}{2}\alpha x)\,dx\,. \tag{A2}$$

The theorem

$$\begin{aligned}\int_0^{\bar{x}} F(x)\sin\left(n\pi\frac{x}{\bar{x}}\right)dx &= \frac{\bar{x}}{\pi}\,S\left\{F\left(\frac{\bar{x}x}{\pi}\right)\right\}\,,\\ \int_0^{\bar{x}} F(x)\cos\left(n\pi\frac{x}{\bar{x}}\right)dx &= \frac{\bar{x}}{\pi}\,C\left\{F\left(\frac{\bar{x}x}{\pi}\right)\right\}\end{aligned} \tag{A3}$$

may be easily proved by introducing the substitution $x' = \pi x/\bar{x}$ in the standard mathematical definition of the Fourier transforms.[62]

Now we make use of the standard results[62]

$$\begin{aligned}S_{\Delta k}\left\{\exp\left(-\frac{\alpha\bar{x}}{2\pi}\,x'\right)\right\} &= \frac{\Delta k'\cdot\pi/\bar{x}}{(\Delta k')^2 + (\frac{1}{2}\alpha)^2}\times[1-(-1)^n\exp(-\tfrac{1}{2}\alpha\bar{x})]\,,\\ C_{\Delta k}\left\{\exp\left(-\frac{\alpha\bar{x}x'}{2\pi}\right)\right\} &= \frac{\alpha\pi/2\bar{x}}{(\Delta k')^2 + (\frac{1}{2}\alpha)^2}\times[1-(-1)^n\exp(-\tfrac{1}{2}\alpha\bar{x})]\,,\end{aligned} \tag{A4}$$

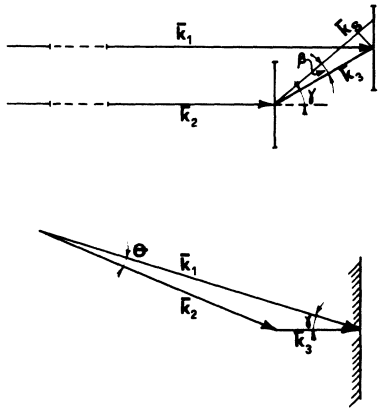

(a)

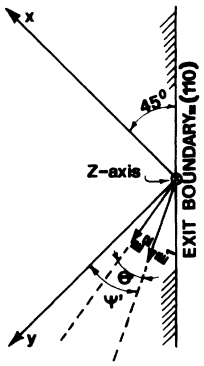

(b)

FIG. 10. (a) Geometrical configuration of the three-wave interaction in the crystal in the experimental conditions of normal emission from the exit boundary, $\varphi = 0$, and quasicollinear kinematics. (b) Crystallographic orientation of the GaP prism used in the experiment [exit boundary coinciding with the (110) plane]. The electric fields of the two interacting transverse optical waves k_1 and k_2 are shown.

$n \equiv \Delta k' \cdot \bar{x}/r$ being a whole number. We assume that n is, in our case, an even number.

In order to simplify the expression on the right-hand side of (A4) we recall the definition of V, that allows us to write $\exp(-\frac{1}{2}\alpha\bar{x}) \simeq [1 - \frac{1}{2}\alpha\bar{x}]$.

Through Eqs. (A2)–(A4) we finally get the result

$$\int_0^{\bar{x}} \exp[(i\Delta k' - \tfrac{1}{2}\alpha)x]\,dx \simeq \frac{\bar{x}\frac{1}{2}\alpha}{\frac{1}{2}\alpha - i\Delta k'} ,$$

which leads, through (A1) and the square-modulus operation, to the Lorentzian function appearing in Eq. (5) of the text.

APPENDIX B

Let us assume an interaction length in the crystal $l \gg \alpha^{-1}$ and consider that $k_1 \sim k_2 \gg k_3$. The angular distributions of the $\vec{k}_1$ and $\vec{k}_2$ vectors in the medium, arising from the effect of the intrinsic divergence and from the focalization of the optical beams, determine two concentric sphere sectors of radii k_1 and k_2. The angle ϑ existing between the vectors $\vec{k}_1$ and $\vec{k}_2$ is always very small and the sphere sectors may be well approximated for our purpose by two plane sectors apart by $k_1 - k_2$. We may assume for simplicity that these plane sectors are parallel in the quasicollinear configuration [cf. Fig. 10(a)]. In a noncollinear scattering condition the polariton wave vector $\vec{k}_3$ makes an angle γ with the direction of $\vec{k}_1$, while the wave vector $\vec{k}_s$ of a slightly non-phase-matched excitation makes an angle $\alpha = \gamma + \beta$ with the same direction. If β is very small, a simple geometrical consideration on two similar rectangular triangles appearing in Fig. 10(a) leads to the expression

$$\Delta = \tan\gamma \sin\beta , \qquad \text{(B1)}$$

Δ being the phase-matching parameter $\Delta \equiv (k_s - k_3)/k_3$ that we have defined in Sec. III. For $\Delta \ll 1$ the intensity of the non-phase-matched field $I_\Delta \propto |E_s|^2$ is related to the corresponding phase-matched intensity I through the equation

$$I_\Delta = I \frac{\delta^2}{\Delta^2 + \delta^2} , \quad \delta = \alpha c/2\omega_3 n_T' \qquad \text{(B2)}$$

owing to Eq. (33). If $\vec{k}_3$ is now made orthogonal to the exit boundary of the crystal, as in our experiment, β becomes the incidence angle φ_s appearing in Eq. (36) and the generalized Snell equations may be applied in order to express I_Δ as function of the emission angle φ:

$$\sin\varphi = n_s \sin\varphi_s \equiv n_T'(1 + \Delta)\sin\varphi_s .$$

Owing to Eq. (B1), we find after some algebra

$$\Delta = \frac{1}{2}\left[\left(1 + \frac{4\tan\gamma\sin\varphi}{n_T'}\right)^{1/2} - 1\right] \sim \frac{\tan\gamma\sin\varphi}{n_T'}$$

for small γ, φ, and $n_T' \gg 1$. Inserting that expression for Δ and $\alpha = 2n_T'\delta\omega_3/c$ in Eq. (B2), we get the Lorentzian factor appearing in Eq. (39). If we now take into account the full spectral width $\bar{\delta}$ of one of the Stokes frequencies, say, ω_1, we may think that the corresponding perturbation of the vector $\vec{k}_1$, equal to $\bar{\delta}k_1/\omega_1$, corresponds to a parallel displacement of the same quantity of one of the plane sectors of Fig. 10(a). A simple geometrical consideration leads to the expression given in the text,

$$[\cos(\varphi_s)_{\bar{\delta}} - \cos(\varphi_s)_0] = \frac{\bar{\delta}}{\omega_1}\,\frac{k_1}{k_3} ,$$

$(\varphi_s)_{\bar{\delta}}$ being the perturbed value of the incidence angle.

The function $f(\gamma, \varphi)$ appearing in Eq. (39) is found by simply inserting the expression of $\Delta(\gamma, \varphi)$ we have just derived in the expression of $n_s = n_T'(1 + \Delta)$ appearing in the generalized Fresnel equation (36).

The function $g(\gamma, \varphi_s, \vartheta)$ is evaluated with reference to Fig. 10(b), showing the orientation of the crystal in our experiment. The direction of the nonlinear polarization vector at the exit surface is parallel to the crystallographic z axis and is given by

$$P_z^{NL}(\omega_3) = d_{zxy}E_{1x}(\omega_1)E_{2y}^*(-\omega_2) + d_{zyx}E_{1y}(\omega_1)E_{2x}^*(-\omega_2) .$$

Owing to the intrinsic permutation symmetry of the susceptibility tensor (Ref. 33, p. 21), $d_{zxy}(\omega_1, -\omega_2) = d_{zyx}(\omega_1, -\omega_2) \equiv d$. The components of the fields are

$$E_{1x} = -E_1 \sin\psi' , \qquad E_{1y} = E_1 \cos\psi' ,$$

$$E_{2x} = -E_2 \sin(\psi' - \vartheta) \simeq -E_2[\sin\psi' - \vartheta\cos\psi'] ,$$

$$E_{2y} = E_2 \cos(\psi' - \vartheta) \simeq E_2[\cos\psi' + \vartheta\sin\psi'] ,$$

with $E_1 = |\vec{E}_1|$, $E_2 = |\vec{E}_2|$, and $\vartheta \ll 1$. The resulting nonlinear polarization is given by

$$P_z^{NL} = -dE_1E_2^*\{\sin2\psi' - \vartheta\cos2\psi'\} .$$

Considering that $\psi' = 45° - \varphi_s - \gamma$, the expression of the nonlinear polarization as a function of the characteristic angles of the interaction, ϑ, γ, and φ_s, is finally given by

$$P_z^{NL}(\omega_3) = -dE_1(\omega_1)E_2^*(-\omega_2) \times [\cos2(\varphi_s + \gamma) - \vartheta\sin2(\varphi_s + \gamma)] . \quad \text{(B3)}$$

The expression $|P_z^{NL}(\vartheta, \gamma, \varphi_s)|^2$ may be now divided by the corresponding one for $\varphi_s = 0$ that is proportional to the ir intensity emitted at $\varphi = 0$. The final expression,

$$g(\vartheta, \gamma, \varphi_s) = |P_z^{NL}(\vartheta, \gamma, \varphi_s)/P_z^{NL}(\vartheta, \gamma, 0)|^2 ,$$

is given in Eq. (40) of the text. We verify that, in the condition of our experiment at $\lambda = 34.6\ \mu$, $g(\vartheta, \gamma, \varphi_s) \approx 1$.

---

*Work supported by CNR.

[1]R. Loudon, Proc. Phys. Soc. (London) 82, 393 (1963).

[2]E. Garmire, F. Pandarese, and C. H. Townes, Phys. Rev. Letters 11, 60 (1963).

[3]Y. R. Shen, Phys. Rev. 138, A1741 (1965).

[4]P. N. Butcher, R. Loudon, and T. P. McLean, Proc. Phys. Soc. (London) 85, 565 (1965).

[5]F. De Martini, J. Appl. Phys. 37, 12 (1966); Nuovo Cimento 51B, 16 (1967).

[6]C. Flytzanis and J. Ducuing, Phys. Rev. 178, 1218 (1969); S. S. Iha and N. Bloembergen, *ibid.* 171, 891 (1968); B. F. Levine, Phys. Rev. Letters 22, 787 (1969).

[7]J. J. Hopfield, Phys. Rev. 112, 1555 (1958).

[8]J. P. Coffinet and F. De Martini, Phys. Rev. Letters 22, 60 (1969).

[9]J. M. Aref'ev, Zh. Eksperim. i Teor. Fiz. Pis'ma v Redaktsiyu 8, 142 (1968) [Sov. Phys. JETP Letters 8, 84 (1968)].

[10]S. K. Kurtz and J. Giordmaine, Phys. Rev. Letters 22, 192 (1969).

[11]J. M. Yarborough *et al.*, App. Phys. Letters 15, 102 (1969); B. C. Johnson *et al.*, *ibid.* 18, 181 (1971).

[12]N. Bloembergen, *Non-Linear Optics* (Benjamin, New York, 1965), p. 105.

[13]C. H. Henry and J. J. Hopfield, Phys. Rev. Letters 15, 964 (1965).

[14]A first account of the present work was reported at the Eighth International Conference on Crystallography, Stony Brook, 1969 (unpublished). See also F. De Martini, Phys. Letters 30A, 319 (1969).

[15]F. Zernicke and P. R. Berman, Phys. Rev. Letters 15, 999 (1965).

[16]M. D. Martin and E. L. Thomas, IEEE J. Quantum Electron. QE-2, 196 (1966).

[17]T. Yajima and K. Inoue, IEEE J. Quantum Electron. QE-5, 140 (1969).

[18]D. W. Faries, K. A. Gehring, P. L. Richards, and Y. R. Shen, Phys. Rev. 180, 363 (1969).

[19]F. Zernicke, Phys. Rev. Letters 22, 931 (1969).

[20]S. Biraud and G. Chartier, Phys. Letters 30A, 177 (1969).

[21]J. A. Giordmaine and R. C. Miller, in *Physics of Quantum Electronics*, edited by P. L. Kelley, B. Lax, and P. E. Tannenwald (McGraw-Hill, New York 1966).

[22]C. H. Henry and C. G. B. Garrett, Phys. Rev. 171, 1058 (1968). We notice that the large number of misprints in this work could make difficult the reading of that useful work. Owing to space limitations we only list here the expressions that need to be corrected. These are Eqs. (2), (3), (8), (18), (27), (29), and (33). The quoted misprints have no consequence on the correctness of the results. However, the frequency dependence of the ratio of the idler flux density to the signal flux density shown in Fig. 2, should exhibit a minimum at $\omega \sim 250$ cm^{-1}.

[23]W. L. Faust and C. H. Henry, Phys. Rev. Letters 17, 1265 (1966); W. L. Faust, C. H. Henry, and R. H. Eick, Phys. Rev. 173, 781 (1968).

[24]M. Born and K. Huang, *Dynamical Theory of Crystal Lattices* (Clarendon, Oxford, 1954), Chap. II.

[25]C. G. B. Garrett, IEEE J. Quantum Electron. QE-4, 70 (1968).

[26]L. I. Shiff, *Quantum Mechanics* (McGraw-Hill, New York, 1968), Chap. 14.

[27]K. Huang, Proc. Roy Soc. (London) A208, 352 (1951).

[28]H. Pelzer, Proc. Roy Soc. (London) A208, 365 (1951).

[29]L. D. Landau and E. M. Lifshitz, *Electrodynamics of Continuous Media* (Pergamon, New York, 1960), p. 253.

[30]R. Loudon, Proc. Roy. Soc. A275, 218 (1963); in *Quantum Optics: International School Enrico E. Fermi, Course XLII*, edited by R. Glauber (Academic, New York, 1969).

[31]J. M. Ziman, *Electrons and Phonons* (Oxford U. P., Oxford, 1960), p. 135.

[32]W. Heitler, *Quantum Theory of Radiation* (Oxford U. P., Oxford, 1954), Sec. 7.

[33]P. N. Butcher, *Nonlinear Optical Phenomena* (Ohio State U. P., Columbus, Ohio, 1965), p. 43, Bulletin 200.

[34]A. Abragam, *The Principles of Nuclear Magnetism* (Oxford U. P., Oxford, 1961), pp. 36 and 44.

[35]F. De Martini (unpublished).

[36]F. De Martini and J. Ducuing, Phys. Rev. Letters 17, 117 (1966); J. Ducuing and F. De Martini, J. Chim. Phys. 1, 209 (1967).

[37]J. Ducuing, C. Joffrin, and J. P. Coffinet, Opt. Commun. 2, 245 (1970).
[38]F. De Martini, J. Ducuing, and G. Hauchecorne, IEEE J. Quantum Electron. QE-4, 67 (1968).
[39]S. R. Hartmann, IEEE J. Quantum Electron. QE-4, 802 (1968).
[40]N. Bloembergen and P. S. Pershan, Phys. Rev. 128, 606 (1962).
[41]M. Born and E. Wolf, *Principles of Optics* (Pergamon, New York, 1964), p. 14.
[42]Equations similar to our Eq. (23) may be found in Ref. 22. However, the equation for $\vec{E}_\omega(\omega_3)$ reported in Ref. 22 lacks the driving term proportional to $\vec{Q}(\omega_3)$.
[43]An expression similar to our Eq. (26) is reported in Ref. 40 with a misprint: The factor depending on p in Eq. (2.5) of Ref. 40 is written as $\vec{p}-\vec{k}_s(\vec{k}_s\cdot\vec{p}/k_T^2)$.
[44]A. S. Barker, Phys. Rev. 165, 917 (1968).
[45]See the work of M. Haas, in *Semiconductors and Semimetals*, edited by R. K. Willardson and A. C. Beer (Academic, New York, 1967), Vol. 3.
[46]F. De Martini (unpublished).
[47]J. A. Giordmaine, Phys. Rev. Letters 8, 19 (1962).
[48]P. D. Maker, R. W. Terhune, M. Nisenhoff, and C. M. Savage, Phys. Rev. Letters 8, 21 (1962).
[49]D. A. Kleinman and W. G. Spitzer, Phys. Rev. 118, 110 (1960).
[50]D. F. Nelson and E. H. Turner, J. Appl. Phys. 39, 3337 (1968).
[51]W. Bond, J. Appl. Phys. 36, 1674 (1965).
[52]H. Welcher, J. Electron. 1, 181 (1955).
[53]F. De Martini, C. H. Townes, R. Gustafson, and P. Kelley, Phys. Rev. 164, 312 (1967).
[54]J. Cooper, Nature 194, 269 (1962).
[55]A. Hadni, J. Phys. (Paris) 24, 694 (1963); A. Hadni, Y. Hanninger, R. Thomas, P. Vergnat, and B. Wyncke, *ibid.* 26, 345 (1965); A. Hadni, R. Thomas, and J. Perrin, J. Appl. Phys. 40, 2740 (1969).
[56]F. Jona and G. Shirane, *Ferroelectric Crystals* (MacMillan, New York, 1962).
[57]A fast pyroelectric detector using $Sr_{1-x}Ba_xNb_2O_6$ crystals has been reported by A. M. Glass, Appl. Phys. Letters 13, 147 (1968).
[58]See the work of E. H. Putley, in *Semiconductors and Semimetals*, edited by R. K. Willardson and A. C. Beer (Academic, New York, 1970), Vol. 5.
[59]The stimulated Raman shifts we assumed for the interpretation of the results of our experiments were those reported by G. Eckhardt *et al.*, Phys. Rev. Letters 9, 455 (1962). These data are in good agreement with the values of the spontaneous Raman shifts reported in G. Herzberg, *Infrared and Raman Spectra of Polyatomic Molecules* (Van Nostrand, New York, 1945).
[60]I. P. Kaminow and E. H. Turner, Appl. Opt. 5, 1612 (1966).
[61]In view of the results of the multiple-oscillator theory that describes the linear dynamical behavior of the lattice in GaP, and that involves a frequency-dependent damping parameter $\Gamma(\omega)$ (see Ref. 44), we can assume that the single-oscillator model in the nonlinear regime is only a first approximation picture of the real behavior of the crystal.
[62]R. V. Churchill, *Modern Operational Mathematics in Engineering* (McGraw-Hill, New York, 1965).

PHYSICAL REVIEW B VOLUME 4, NUMBER 12 15 DECEMBER 1971

Determination of Absolute Signs of Microwave Nonlinear Susceptibilities

M. A. Pollack and E. H. Turner
Bell Telephone Laboratories, Holmdel, New Jersey 07733
(Received 28 June 1971)

The sign of the microwave nonlinear susceptibility has been found for the first time for a number of acentric crystals. The method used determines the absolute sign without recourse to a comparison crystal. Using known signs of piezoelectric coefficients to specify crystal orientation, all of the nonlinear susceptibilities measured are negative. Predictions of signs and magnitudes of some coefficients in pyroelectric crystals are also made.

INTRODUCTION

Complete specification of a nonlinear susceptibility requires not only that its magnitude be known but also that an algebraic sign related to a defined positive direction in the crystal be given. We describe here a method of finding the absolute signs of microwave nonlinear susceptibility coefficients (d^m) and relate these to positive axes found by piezoelectric tests. We also present the sign results for some crystals in order to complement the recent[1] measurements of the d^m magnitudes. These results, together with recent determinations of the signs of electro-optic[1-3] (d^{∞}) and nonlinear optical[3,4] (d^0) susceptibilities allow further characterization of materials in terms of Garrett's four-parameter anharmonic-oscillator model.[1,5] Additionally, in pyroelectric crystals, predictions can be made of magnitudes and signs of some tensor components of d^m other than those directly measured.

The determination[4] of d^0 signs involves comparison with a known crystal. This, in turn, requires that the sign of d^{∞} for at least one crystal be determined[6] and that its behavior be followed as the modulation frequency is increased through the lattice resonance region.[7] The d^{∞} sign determination[2] is also a comparison using a crystal of known[6] sign. In our method of finding d^m signs, however, each

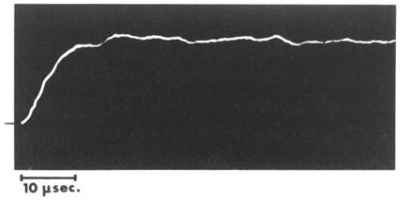

FIG. 6. Pyroelectric detector signal corresponding to the detection of a 1-μW 20-nsec ir pulse emitted at $\lambda = 34.6\ \mu$.